

NOAA Atlas NESDIS 68



WORLD OCEAN ATLAS 2009
Volume 1: Temperature

Silver Spring, MD
March 2010

U.S. DEPARTMENT OF COMMERCE
National Oceanic and Atmospheric Administration
National Environmental Satellite, Data, and Information Service

National Oceanographic Data Center

Additional copies of this publication, as well as information about NODC data holdings and services, are available upon request directly from NODC.

National Oceanographic Data Center
User Services Team
NOAA/NESDIS E/OC1
SSMC III, 4th floor
1315 East-West Highway
Silver Spring, MD 20910-3282

Telephone: (301) 713-3277

Fax: (301) 713-3302

E-mail: NODC.Services@noaa.gov

NODC URL: <http://www.nodc.noaa.gov/>

For updates on the data, documentation, and additional information about the WOA09 please refer to:

<http://www.nodc.noaa.gov/OC5/indprod.html>

This document should be cited as:

Locarnini, R. A., A. V. Mishonov, J. I. Antonov, T. P. Boyer, H. E. Garcia, O. K. Baranova, M. M. Zweng, and D. R. Johnson, 2010. *World Ocean Atlas 2009, Volume 1: Temperature*. S. Levitus, Ed., NOAA Atlas NESDIS 68, U.S. Government Printing Office, Washington, D.C., 184 pp.

This document is available on line at <http://www.nodc.noaa.gov/OC5/indprod.html>.

NOAA Atlas NESDIS 68

WORLD OCEAN ATLAS 2009
Volume 1: Temperature

Ricardo A. Locarnini, Alexey V. Mishonov, John I. Antonov,
Timothy P. Boyer, Hernan E. Garcia, Olga K. Baranova, Melissa M.
Zweng, and Daphne R. Johnson

Editor: Sydney Levitus

Ocean Climate Laboratory
National Oceanographic Data Center

Silver Spring, Maryland
March, 2010



U.S. DEPARTMENT OF COMMERCE
Gary Locke, Secretary

National Oceanic and Atmospheric Administration
Jane Lubchenco,
Under Secretary of Commerce for Oceans and Atmosphere

National Environmental Satellite, Data and Information Service
Mary E. Kicza, Assistant Administrator

Table of Contents

Table of Contents	i
List of Figures	ii
List of Tables	ii
List of Maps in the Appendices	iii
Preface	viii
Acknowledgments	ix
ABSTRACT	1
1. INTRODUCTION	1
2. DATA AND DATA DISTRIBUTION	2
2.1. Data sources	2
2.2. Data quality control.....	3
2.2.1. Duplicate elimination.....	4
2.2.2. Range and gradient checks	4
2.2.3. Statistical checks	4
2.2.4. Static stability check	5
2.2.5. Subjective flagging of data.....	5
2.2.6. Representativeness of the data.....	6
2.2.7. XBT drop rate error correction	6
3. DATA PROCESSING PROCEDURES	7
3.1. Vertical interpolation to standard levels	7
3.2. Methods of analysis	7
3.2.1. Overview	7
3.2.2. Derivation of Barnes (1964) weight function	9
3.2.3. Derivation of Barnes (1964) response function.....	10
3.2.4. Choice of response function.....	11
3.2.5. First-guess field determination	12
3.3. Choice of objective analysis procedures.....	12
3.4. Choice of spatial grid	13
3.5. Stabilization of Temperature and Salinity Climatologies.....	13
4. RESULTS	14
4.1. Computation of annual and seasonal fields	14
4.2. Available statistical fields	14
4.3. Obtaining WOA09 fields online	15
5. SUMMARY	15
6. FUTURE WORK	16
7. REFERENCES	16
8. APPENDICES	28
8.1. Appendix A: Stabilization of Temperature and Salinity Climatologies	28
8.2. Appendix B: Example of Stabilization	33
8.3. Appendix C: Maps of data distribution and climatological mean temperature for the annual compositing period for selected standard depth levels.....	39

- 8.4. Appendix D: Maps of data distribution, climatological mean temperature, and difference from annual mean for each seasonal compositing period for selected standard depth levels... 39
- 8.5. Appendix E: Maps of data distribution, climatological mean temperature, and difference from annual mean for each monthly compositing period for selected standard depth levels... 39

List of Figures

- Figure 1.** Response function of the WOA09, WOA05, WOA01, WOA98, WOA94, and Levitus (1982) objective analysis schemes..... 26
- Figure 2.** Scheme used in computing annual, seasonal, and monthly objectively analyzed means for temperature. The final monthly, seasonal, and annual climatologies were density stabilized – see section 3.5..... 27

List of Tables

- Table 1.** Descriptions of climatologies for temperature in WOA09. The standard depth levels are shown in Table 3..... 21
- Table 2.** Descriptions of datasets in WOD09 used to calculate the temperature climatologies.. 21
- Table 3.** Acceptable distances (m) for defining interior and exterior values used in the Reiniger-Ross scheme for interpolating observed level data to standard levels..... 22
- Table 4.** Response function of the objective analysis scheme as a function of wavelength for WOA09 and earlier analyses. Response function is normalized to 1.0..... 23
- Table 5.** Basins defined for objective analysis and the shallowest standard depth level for which each basin is defined..... 24
- Table 6.** Objective and statistical data fields calculated as part of WOA09 (✓ denotes field was calculated and is publicly available)..... 25

List of Maps in the Appendices

Appendix C: Maps of data distribution and climatological mean temperature for the annual compositing period for selected standard depth levels (Pages 41 to 64).

Fig. C1. Annual temperature observations at the surface	41
Fig. C2. Annual temperature observations at 50 m. depth.....	41
Fig. C3. Annual temperature observations at 75 m. depth.....	42
Fig. C4. Annual temperature observations at 100 m. depth.....	42
Fig. C5. Annual temperature observations at 150 m. depth.....	43
Fig. C6. Annual temperature observations at 200 m. depth.....	43
Fig. C7. Annual temperature observations at 250 m. depth.....	44
Fig. C8. Annual temperature observations at 400 m. depth.....	44
Fig. C9. Annual temperature observations at 500 m. depth.....	45
Fig. C10. Annual temperature observations at 700 m. depth.....	45
Fig. C11. Annual temperature observations at 1000 m. depth.....	46
Fig. C12. Annual temperature observations at 1500 m. depth.....	46
Fig. C13. Annual temperature observations at 2000 m. depth.....	47
Fig. C14. Annual temperature observations at 2500 m. depth.....	47
Fig. C15. Annual temperature observations at 3000 m. depth.....	48
Fig. C16. Annual temperature observations at 4000 m. depth.....	48
Fig. C17. Annual temperature [°C] at the surface.	49
Fig. C18. Annual temperature [°C] at 50 m. depth.....	50
Fig. C19. Annual temperature [°C] at 75 m. depth.....	51
Fig. C20. Annual temperature [°C] at 100 m. depth.....	52
Fig. C21. Annual temperature [°C] at 150 m. depth.....	53
Fig. C22. Annual temperature [°C] at 200 m. depth.....	54
Fig. C23. Annual temperature [°C] at 250 m. depth.....	55
Fig. C24. Annual temperature [°C] at 400 m. depth.....	56
Fig. C25. Annual temperature [°C] at 500 m. depth.....	57
Fig. C26. Annual temperature [°C] at 700 m. depth.....	58
Fig. C27. Annual temperature [°C] at 1000 m. depth.....	59
Fig. C28. Annual temperature [°C] at 1500 m. depth.....	60
Fig. C29. Annual temperature [°C] at 2000 m. depth.....	61
Fig. C30. Annual temperature [°C] at 2500 m. depth.....	62
Fig. C31. Annual temperature [°C] at 3000 m. depth.....	63
Fig. C32. Annual temperature [°C] at 4000 m. depth.....	64

Appendix D: Maps of data distribution, climatological mean temperature, and difference from annual mean for each seasonal compositing period for selected standard depth levels (Pages 65 to 124).

Fig. D1. Winter (Jan.-Mar.) temperature observations at the surface.....	65
Fig. D2. Winter (Jan.-Mar.) temperature observations at 50 m. depth.....	65
Fig. D3. Winter (Jan.-Mar.) temperature observations at 75 m. depth.....	66

Fig. D4. Winter (Jan.-Mar.) temperature observations at 100 m. depth.....	66
Fig. D5. Winter (Jan.-Mar.) temperature observations at 150 m. depth.....	67
Fig. D6. Winter (Jan.-Mar.) temperature observations at 250 m. depth.....	67
Fig. D7. Spring (Apr.-Jun.) temperature observations at the surface.....	68
Fig. D8. Spring (Apr.-Jun.) temperature observations at 50 m. depth.....	68
Fig. D9. Spring (Apr.-Jun.) temperature observations at 75 m. depth.....	69
Fig. D10. Spring (Apr.-Jun.) temperature observations at 100 m. depth.....	69
Fig. D11. Spring (Apr.-Jun.) temperature observations at 150 m. depth.....	70
Fig. D12. Spring (Apr.-Jun.) temperature observations at 250 m. depth.....	70
Fig. D13. Summer (Jul.-Sep.) temperature observations at the surface.....	71
Fig. D14. Summer (Jul.-Sep.) temperature observations at 50 m. depth.....	71
Fig. D15. Summer (Jul.-Sep.) temperature observations at 75 m. depth.....	72
Fig. D16. Summer (Jul.-Sep.) temperature observations at 100 m. depth.....	72
Fig. D17. Summer (Jul.-Sep.) temperature observations at 150 m. depth.....	73
Fig. D18. Summer (Jul.-Sep.) temperature observations at 250 m. depth.....	73
Fig. D19. Fall (Oct.-Dec.) temperature observations at the surface.....	74
Fig. D20. Fall (Oct.-Dec.) temperature observations at 50 m. depth.....	74
Fig. D21. Fall (Oct.-Dec.) temperature observations at 75 m. depth.....	75
Fig. D22. Fall (Oct.-Dec.) temperature observations at 100 m. depth.....	75
Fig. D23. Fall (Oct.-Dec.) temperature observations at 150 m. depth.....	76
Fig. D24. Fall (Oct.-Dec.) temperature observations at 250 m. depth.....	76
Fig. D25. Winter (Jan.-Mar.) temperature [°C] at the surface.....	77
Fig. D26. Winter (Jan.-Mar.) minus annual temperature [°C] at the surface.....	78
Fig. D27. Winter (Jan.-Mar.) temperature [°C] at 50 m. depth.....	79
Fig. D28. Winter (Jan.-Mar.) minus annual temperature [°C] at 50 m. depth.....	80
Fig. D29. Winter (Jan.-Mar.) temperature [°C] at 75 m. depth.....	81
Fig. D30. Winter (Jan.-Mar.) minus annual temperature [°C] at 75 m. depth.....	82
Fig. D31. Winter (Jan.-Mar.) temperature [°C] at 100 m. depth.....	83
Fig. D32. Winter (Jan.-Mar.) minus annual temperature [°C] at 100 m. depth.....	84
Fig. D33. Winter (Jan.-Mar.) temperature [°C] at 150 m. depth.....	85
Fig. D34. Winter (Jan.-Mar.) minus annual temperature [°C] at 150 m. depth.....	86
Fig. D35. Winter (Jan.-Mar.) temperature [°C] at 250 m. depth.....	87
Fig. D36. Winter (Jan.-Mar.) minus annual temperature [°C] at 250 m. depth.....	88
Fig. D37. Spring (Apr.-Jun.) temperature [°C] at the surface.....	89
Fig. D38. Spring (Apr.-Jun.) minus annual temperature [°C] at the surface.....	90
Fig. D39. Spring (Apr.-Jun.) temperature [°C] at 50 m. depth.....	91
Fig. D40. Spring (Apr.-Jun.) minus annual temperature [°C] at 50 m. depth.....	92
Fig. D41. Spring (Apr.-Jun.) temperature [°C] at 75 m. depth.....	93
Fig. D42. Spring (Apr.-Jun.) minus annual temperature [°C] at 75 m. depth.....	94
Fig. D43. Spring (Apr.-Jun.) temperature [°C] at 100 m. depth.....	95
Fig. D44. Spring (Apr.-Jun.) minus annual temperature [°C] at 100 m. depth.....	96
Fig. D45. Spring (Apr.-Jun.) temperature [°C] at 150 m. depth.....	97
Fig. D46. Spring (Apr.-Jun.) minus annual temperature [°C] at 150 m. depth.....	98
Fig. D47. Spring (Apr.-Jun.) temperature [°C] at 250 m. depth.....	99
Fig. D48. Spring (Apr.-Jun.) minus annual temperature [°C] at 250 m. depth.....	100
Fig. D49. Summer (Jul.-Sep.) temperature [°C] at the surface.....	101

Fig. D50. Summer (Jul.-Sep.) minus annual temperature [°C] at the surface.	102
Fig. D51. Summer (Jul.-Sep.) temperature [°C] at 50 m. depth.	103
Fig. D52. Summer (Jul.-Sep.) minus annual temperature [°C] at 50 m. depth.	104
Fig. D53. Summer (Jul.-Sep.) temperature [°C] at 75 m. depth.	105
Fig. D54. Summer (Jul.-Sep.) minus annual temperature [°C] at 75 m. depth.	106
Fig. D55. Summer (Jul.-Sep.) temperature [°C] at 100 m. depth.	107
Fig. D56. Summer (Jul.-Sep.) minus annual temperature [°C] at 100 m. depth.	108
Fig. D57. Summer (Jul.-Sep.) temperature [°C] at 150 m. depth.	109
Fig. D58. Summer (Jul.-Sep.) minus annual temperature [°C] at 150 m. depth.	110
Fig. D59. Summer (Jul.-Sep.) temperature [°C] at 250 m. depth.	111
Fig. D60. Summer (Jul.-Sep.) minus annual temperature [°C] at 250 m. depth.	112
Fig. D61. Fall (Oct.-Dec.) temperature [°C] at the surface.	113
Fig. D62. Fall (Oct.-Dec.) minus annual temperature [°C] at the surface.	114
Fig. D63. Fall (Oct.-Dec.) temperature [°C] at 50 m. depth.	115
Fig. D64. Fall (Oct.-Dec.) minus annual temperature [°C] at 50 m. depth.	116
Fig. D65. Fall (Oct.-Dec.) temperature [°C] at 75 m. depth.	117
Fig. D66. Fall (Oct.-Dec.) minus annual temperature [°C] at 75 m. depth.	118
Fig. D67. Fall (Oct.-Dec.) temperature [°C] at 100 m. depth.	119
Fig. D68. Fall (Oct.-Dec.) minus annual temperature [°C] at 100 m. depth.	120
Fig. D69. Fall (Oct.-Dec.) temperature [°C] at 150 m. depth.	121
Fig. D70. Fall (Oct.-Dec.) minus annual temperature [°C] at 150 m. depth.	122
Fig. D71. Fall (Oct.-Dec.) temperature [°C] at 250 m. depth.	123
Fig. D72. Fall (Oct.-Dec.) minus annual temperature [°C] at 250 m. depth.	124

Appendix E: Maps of data distribution, climatological mean temperature, and difference from annual mean for each monthly compositing period for selected standard depth levels (Pages 125 to 184).

Fig. E1. January temperature observations at the surface.	125
Fig. E2. January temperature observations at 75 m. depth.	125
Fig. E3. February temperature observations at the surface.	126
Fig. E4. February temperature observations at 75 m. depth.	126
Fig. E5. March temperature observations at the surface.	127
Fig. E6. March temperature observations at 75 m. depth.	127
Fig. E7. April temperature observations at the surface.	128
Fig. E8. April temperature observations at 75 m. depth.	128
Fig. E9. May temperature observations at the surface.	129
Fig. E10. May temperature observations at 75 m. depth.	129
Fig. E11. June temperature observations at the surface.	130
Fig. E12. June temperature observations at 75 m. depth.	130
Fig. E13. July temperature observations at the surface.	131
Fig. E14. July temperature observations at 75 m. depth.	131
Fig. E15. August temperature observations at the surface.	132
Fig. E16. August temperature observations at 75 m. depth.	132
Fig. E17. September temperature observations at the surface.	133
Fig. E18. September temperature observations at 75 m. depth.	133
Fig. E19. October temperature observations at the surface.	134

Fig. E20. October temperature observations at 75 m. depth.....	134
Fig. E21. November temperature observations at the surface.	135
Fig. E22. November temperature observations at 75 m. depth.....	135
Fig. E23. December temperature observations at the surface.....	136
Fig. E24. December temperature observations at 75 m. depth.	136
Fig. E25. January mean temperature [°C] at the surface.	137
Fig. E26. January minus annual temperature [°C] at the surface.	138
Fig. E27. January mean temperature [°C] at 75 m. depth.....	139
Fig. E28. January minus annual temperature [°C] at 75 m. depth.....	140
Fig. E29. February mean temperature [°C] at the surface.	141
Fig. E30. February minus annual temperature [°C] at the surface.	142
Fig. E31. February mean temperature [°C] at 75 m. depth.....	143
Fig. E32. February minus annual temperature [°C] at 75 m. depth.....	144
Fig. E33. March mean temperature [°C] at the surface.	145
Fig. E34. March minus annual temperature [°C] at the surface.	146
Fig. E35. March mean temperature [°C] at 75 m. depth.....	147
Fig. E36. March minus annual temperature [°C] at 75 m. depth.....	148
Fig. E37. April mean temperature [°C] at the surface.	149
Fig. E38. April minus annual temperature [°C] at the surface.....	150
Fig. E39. April mean temperature [°C] at 75 m. depth.....	151
Fig. E40. April minus annual temperature [°C] at 75 m. depth.....	152
Fig. E41. May mean temperature [°C] at the surface.	153
Fig. E42. May minus annual temperature [°C] at the surface.....	154
Fig. E43. May mean temperature [°C] at 75 m. depth.....	155
Fig. E44. May minus annual temperature [°C] at 75 m. depth.....	156
Fig. E45. June mean temperature [°C] at the surface.	157
Fig. E46. June minus annual temperature [°C] at the surface.....	158
Fig. E47. June mean temperature [°C] at 75 m. depth.....	159
Fig. E48. June minus annual temperature [°C] at 75 m. depth.....	160
Fig. E49. July mean temperature [°C] at the surface.	161
Fig. E50. July minus annual temperature [°C] at the surface.	162
Fig. E51. July mean temperature [°C] at 75 m. depth.	163
Fig. E52. July minus annual temperature [°C] at 75 m. depth.....	164
Fig. E53. August mean temperature [°C] at the surface.	165
Fig. E54. August minus annual temperature [°C] at the surface.	166
Fig. E55. August mean temperature [°C] at 75 m. depth.....	167
Fig. E56. August minus annual temperature [°C] at 75 m. depth.....	168
Fig. E57. September mean temperature [°C] at the surface.....	169
Fig. E58. September minus annual temperature [°C] at the surface.....	170
Fig. E59. September mean temperature [°C] at 75 m. depth.....	171
Fig. E60. September minus annual temperature [°C] at 75 m. depth.	172
Fig. E61. October mean temperature [°C] at the surface.....	173
Fig. E62. October minus annual temperature [°C] at the surface.....	174
Fig. E63. October mean temperature [°C] at 75 m. depth.	175
Fig. E64. October minus annual temperature [°C] at 75 m. depth.	176
Fig. E65. November mean temperature [°C] at the surface.....	177

Fig. E66. November minus annual temperature [°C] at the surface.	178
Fig. E67. November mean temperature [°C] at 75 m. depth.	179
Fig. E68. November minus annual temperature [°C] at 75 m. depth.....	180
Fig. E69. December mean temperature [°C] at the surface.	181
Fig. E70. December minus annual temperature [°C] at the surface.....	182
Fig. E71. December mean temperature [°C] at 75 m. depth.....	183
Fig. E72. December minus annual temperature [°C] at 75 m. depth.....	184

Preface

The oceanographic analyses described by this atlas series expand on earlier works, *e.g.*, the *World Ocean Atlas 2005* (WOA05), the *World Ocean Atlas 2001* (WOA01), *World Ocean Atlas 1998* (WOA98), *World Ocean Atlas 1994* (WOA94) and *Climatological Atlas of the World Ocean* (Levitus, 1982). Previously published oceanographic objective analyses have proven to be of great utility to the oceanographic, climate research, and operational environmental forecasting communities. Such analyses are used as boundary and/or initial conditions in numerical ocean circulation models and atmosphere-ocean models, for verification of numerical simulations of the ocean, as a form of “sea truth” for satellite measurements such as altimetric observations of sea surface height, for computation of nutrient fluxes by Ekman transport, and for planning oceanographic expeditions.

We continue preparing climatological analyses on a one-degree grid. This is because higher resolution analyses are not justified for all the variables we are working with and we wish to produce a set of analyses for which all variables have been analyzed in the same manner. High-resolution analyses as typified by the work of Boyer *et al.* (2004) will be published separately.

In the acknowledgment section of this publication we have expressed our view that creation of global ocean profile and plankton databases and analyses are only possible through the cooperation of scientists, data managers, and scientific administrators throughout the international scientific community. I would also like to thank my colleagues and the staff of the Ocean Climate Laboratory of NODC for their dedication to the project leading to publication of this atlas series. Their integrity and thoroughness have made this database possible. It is my belief that the development and management of national and international oceanographic data archives is best performed by scientists who are actively working with the historical data.

Sydney Levitus
National Oceanographic Data Center
Silver Spring, MD
March 2010

Acknowledgments

This work was made possible by a grant from the NOAA Climate and Global Change Program which enabled the establishment of a research group at the National Oceanographic Data Center. The purpose of this group is to prepare research quality oceanographic databases, as well as to compute objective analyses of, and diagnostic studies based on, these databases. Support is now from base funds and from the NOAA Climate Program Office.

The data on which this atlas is based are in *World Ocean Database 2009* and are distributed on-line and on DVD by NODC/WDC. Many data were acquired as a result of the IOC/IODE *Global Oceanographic Data Archaeology and Rescue* (GODAR) project, and the IOC/IODE *World Ocean Database* project (WOD). At NODC/WDC, data archaeology and rescue projects were supported with funding from the NOAA Environmental Science Data and Information Management (ESDIM) Program and the NOAA Climate and Global Change Program which has included support from NASA and DOE. Support for some of the regional IOC/GODAR meetings was provided by the Marine Science and Technology (MAST) program of the European Union. The European Community has also provided support for the Mediterranean Data Archeology and Rescue (MEDAR/MEDATLAS) project which has resulted in the inclusion of substantial amounts of ocean profile data from the Mediterranean Sea. Additional Black Sea data have been acquired as a result of a NATO sponsored project.

We acknowledge the scientists, technicians, and programmers who have collected and processed data, those individuals who have submitted data to national and regional data centers as well as the managers and staff at the various data centers. We thank our colleagues at the NODC. Their efforts have made this and similar works possible.

WORLD OCEAN ATLAS 2009

Volume 1: Temperature

ABSTRACT

This atlas consists of a description of data analysis procedures and horizontal maps of annual, seasonal, and monthly climatological distribution fields of temperature at selected standard depth levels of the world ocean on a one-degree latitude-longitude grid. The aim of the maps is to illustrate large-scale characteristics of the distribution of ocean temperature. The fields used to generate these climatological maps were computed by objective analysis of all scientifically quality-controlled historical temperature data in the *World Ocean Database 2009*. Maps are presented for climatological composite periods (annual, seasonal, monthly, seasonal and monthly difference fields from the annual mean field, and the number of observations) at selected standard depths.

1. INTRODUCTION

This atlas is part of the *World Ocean Atlas 2009* (WOA09) series. The WOA09 series include analysis for temperature (this atlas), salinity (Antonov *et al.*, 2010), dissolved oxygen, Apparent Oxygen Utilization, and oxygen saturation (Garcia *et al.*, 2010a), and dissolved inorganic nutrients (Garcia *et al.*, 2010b). Presented here are annual, seasonal, and monthly climatologies and related statistical fields for temperature. Climatologies are here defined as mean oceanographic fields at selected standard depth levels based on the objective analysis of historical oceanographic profiles and select surface-only data. A profile is defined as a set of measurements for a single variable (temperature, salinity, *etc.*) at discrete depths taken as an instrument drops or rises vertically in the water column. Temperature and salinity climatologies are the average of five “decadal” climatologies for the following time periods: 1955-1964, 1965-1974, 1975-1984, 1985-1994, and 1995-2006, while oxygen and nutrients climatologies use all

available data regardless of year of observation (“all-data” climatology). The annual “all-data” climatology was calculated using all data regardless of the month in which the observation was made. Seasonal “all-data” climatologies were calculated using only data from the defined season (regardless of year). The seasons are here defined as follows. Winter is defined as the months of January, February, and March. Spring is defined as April, May, and June. Summer is defined as July, August, and September. Fall is defined as October, November, and December. Monthly “all-data” climatologies were calculated using data only from the given month regardless of the day of the month in which the observation was made. These monthly “all-data” climatologies were used as the first guess for each “decadal” climatology.

The temperature data used are available from the National Oceanographic Data Center (NODC) and World Data Center (WDC) for Oceanography, Silver Spring, Maryland. Large volumes of data have been acquired as a result of the fulfillment

of several data management projects including:

- a) the Intergovernmental Oceanographic Commission (IOC) Global Oceanographic Data Archaeology and Rescue (GODAR) project (Levitus *et al.*, 2005);
- b) the IOC World Ocean Database project (WOD);
- c) the IOC Global Temperature Salinity Profile project (GTSP) (IOC, 1998).

The temperature data used in the WOA09 have been analyzed in a consistent, objective manner on a one-degree latitude-longitude grid at standard depth levels from the surface to a maximum depth of 5500 m. The procedures for “all-data” climatologies are identical to those used in the *World Ocean Atlas 2005* (WOA05) series (Locarnini *et al.*, 2006; Antonov *et al.*, 2006; Garcia *et al.*, 2006 a, b), *World Ocean Atlas 2001* (WOA01) series (Stephens *et al.*, 2002; Boyer *et al.*, 2002; Locarnini *et al.*, 2002; Conkright *et al.*, 2002), and *World Ocean Atlas 1998* (WOA98) series (Antonov *et al.*, 1998 a, b, c; Boyer *et al.*, 1998 a, b, c; Conkright *et al.*, 1998 a, b, c; O’Brien *et al.*, 1998 a, b, c). Slightly different procedures were followed in earlier analyses (Levitus, 1982; *World Ocean Atlas 1994* series [WOA94, Levitus *et al.*, 1994; Levitus and Boyer, 1994 a, b; Conkright *et al.*, 1994]). This analysis differs from WOA05 by presenting the monthly climatological fields that are the average of five “decadal” climatologies.

Objective analyses shown in this atlas are limited by the nature of the temperature data base (data are non-uniform in both space and time), characteristics of the objective analysis techniques, and the grid used. These limitations and characteristics are discussed below.

Since the publication of WOA05, substantial amounts of additional historical temperature data have become available. However, even with these additional data, we are still hampered in a number of ways by a lack of data. In some areas, quality control is made difficult by the limited number of data collected in these areas. Data may exist in an area for only one season, thus precluding any representative annual analysis. In some areas there may be a reasonable spatial distribution of data points on which to base an analysis, but there may be only a few (perhaps only one) data values in each one-degree latitude-longitude square.

This atlas is divided into sections. We begin by describing the data sources and data distribution (Section 2). Then we describe the general data processing procedures (Section 3), the results (Section 4), summary (Section 5), and future work (Section 6). After the references (Section 7), the appendices of this atlas (Section 8) include descriptions and examples of the stabilization of the temperature and salinity climatologies, and global horizontal maps for temperature at selected standard depth levels.

2. DATA AND DATA DISTRIBUTION

Data sources and quality control procedures are briefly described below. For further information on the data sources used in WOA09 refer to the *World Ocean Database 2009* (WOD09, Boyer *et al.*, 2009). The quality control procedures used in preparation of these analyses are described by Johnson *et al.* (2009).

2.1. Data sources

Historical oceanographic temperature profile data from bottle samples (Reversing thermometers), Mechanical Bathymograph (MBT), ship-deployed

Conductivity-Temperature-Depth (CTD) package, Digital Bathythermograph (DBT), Expendable Bathythermograph (XBT), profiling float, moored and drifting buoys, gliders, and undulating oceanographic recorder (UOR) profiles used in this project were obtained from the NODC/WDC archives and include all data gathered as a result of the GODAR and WOD projects.

To understand the procedures for taking individual oceanographic observations and constructing climatological fields, definition of the terms “standard level data” and “observed level data” are necessary. We refer to the actual measured value of an oceanographic variable *in situ* (Latin for “in place”) as an “observation”, and to the depth at which such a measurement was made as the “observed level depth.” We refer to such data as “observed level data.” Before the development of oceanographic instrumentation that measures at high frequencies along the vertical profile, oceanographers often attempted to make measurements at selected “standard levels” in the water column. Sverdrup *et al.* (1942) presented the suggestions of the International Association of Physical Oceanography (IAPSO) as to which depths oceanographic measurements should be made or interpolated to for analysis. Different nations or institutions have a slightly different set of standard depth levels defined. For many purposes, including preparation of the present climatologies, observed level data are interpolated to standard depth levels, if observations did not occur at the desired standard depths. The levels at which the temperature climatologies were calculated are given in Table 1. Table 2 describes the datasets used to calculate the climatologies. Table 3 shows the depths of each standard depth level. Section 3.1 discusses the vertical interpolation procedures used in our work.

2.2. Data quality control

Quality control of the temperature data is a major task, the difficulty of which is directly related to lack of data and metadata (for some areas) upon which to base statistical checks. Consequently certain empirical criteria were applied - see sections 2.2.1 through 2.2.4, and as part of the last processing step, subjective judgment was used - see sections 2.2.5 and 2.2.6. Individual temperature data, and in some cases entire profiles or all profiles for individual cruises, have been flagged and not used further because these data produced features that were judged to be non-representative or questionable. As part of our work, we have made available WOD09 which contains both observed levels profile data and standard depth level profile data with various quality control flags applied. The flags mark individual measurements, or entire profiles which were not used in the next step of the procedure, either interpolation to standard depth levels for observed level data or calculation of statistical means in the case of standard depth level data. Our knowledge of the variability of the world ocean now includes a greater appreciation and understanding of the ubiquity of eddies, rings, and lenses in some parts of the world ocean as well as interannual and interdecadal variability of water mass properties associated with modal variability of the atmosphere such as the North Atlantic Oscillation (NAO) and El Niño Southern Ocean Oscillation (ENSO). Therefore, we have simply flagged data, not eliminating them from the WOD09. Thus, individual investigators can make their own decision regarding the representativeness of the data. Investigators studying the distribution of features such as eddies will be interested in those data that we may regard as unrepresentative for the preparation of the analyses shown in this atlas.

2.2.1. Duplicate elimination

Because temperature data are received from many sources, sometimes the same data set is received at NODC/WDC more than once but with slightly different time and/or position and/or data values, and hence are not easily identified as duplicate stations. Therefore, to eliminate the repetitive data values our databases were checked for the presence of exact and “near” exact replicates using eight different criteria. The first checks involve identifying stations with exact position/date/time and data values; the next checks involve offsets in position/date/time. Profiles identified as duplicates in the checks with a large offset were individually verified to ensure they were indeed duplicate profiles.

All but one profile from each set of replicate profiles were eliminated at the first step of our processing.

2.2.2. Range and gradient checks

Range checking (*i.e.*, checking whether a temperature value is within preset minimum and maximum values as a function of depth and ocean region) was performed on all temperature values as a first quality control check to flag and withhold from further use the relatively few values that were grossly outside expected oceanic ranges. Range checks were prepared for individual regions of the world ocean. Johnson *et al.* (2009) and Boyer and Levitus (1994) detail the quality control procedures. Range tables showing the temperature ranges selected for each basin and depth can be found in Johnson *et al.* (2009).

A check as to whether excessive vertical gradients occur in the data has been performed for each variable in WOD09 both in terms of *positive* and negative gradients. See Johnson *et al.* (2009) for limits for excessive gradients for temperature.

2.2.3. Statistical checks

Statistical checks were performed as follows. All data for temperature (irrespective of year), at each standard depth level, were averaged within five-degree latitude-longitude squares to produce a record of the number of observations, mean, and standard deviation in each square. Statistics were computed for the annual, seasonal, and monthly compositing periods. Below 50 m depth, if data were more than three standard deviations from the mean, the data were flagged and withheld from further use in objective analyses. Above 50 m depth, a five-standard-deviation criterion was used in five-degree squares that contained any land area. In selected five-degree squares that are close to land areas, a four-standard-deviation check was used. In all other squares a three-standard-deviation criterion was used for the 0-50 m depth layer. For standard depth levels situated directly above the bottom, a four-standard-deviation criterion was used.

The *reason* for the weaker standard deviation criterion in coastal and near-coastal regions is the exceptionally large variability in the coastal five-degree square statistics for some variables. Frequency distributions of some variables in some coastal regions are observed to be skewed or bimodal. Thus to avoid eliminating of possibly good data in highly variable environments, the standard deviation criteria were broadened.

The total number of measurements in each profile, as well as the total number of *temperature* observations exceeding the criterion, were recorded. If more than two observations in a profile were found to exceed the standard deviation criterion, then the entire profile was flagged. This check was imposed after tests indicated that surface data from particular casts (which upon inspection appeared to be erroneous)

were being flagged but deeper data were not. Other situations were found where erroneous data from the deeper portion of a cast were flagged, while near-surface data from the same cast were not flagged because of larger natural variability in surface layers. One reason for this was the decrease of the number of observations with depth and the resulting change in sample statistics. The standard-deviation check was applied twice to the data set for each compositing period.

In summary, first the five-degree square statistics were computed, and the data flagging procedure described above was used to provide a preliminary data set. Next, new five-degree-square statistics were computed from this preliminary data set and used with the same statistical check to produce a new, “clean” data set. The reason for applying the statistical check twice was to flag (and withhold from further use), in the first round, any grossly erroneous or non-representative data from the data set that would artificially increase the variances. The second check is then more effective in identifying smaller, but non-representative, observations.

2.2.4. Static stability check

Each cast containing both temperature and salinity was checked for static stability as defined by Hesselberg and Sverdrup (1914). Neumann and Pierson (1966, p. 139) reviewed this definition. The computation is a “local” one in the sense that adiabatic displacements between adjacent temperature-salinity measurements in the vertical are considered rather than displacements to the sea surface. Lynn and Reid (1968) discussed the reasons for use of the local stability computation. The procedure for computation follows that used by Lynn and Reid (1968) and is given by:

$$E = \lim_{\partial z \rightarrow 0} \frac{1}{\rho_0} \frac{\delta \rho}{\partial z}$$

in which: $\rho_0 = 1.02 \cdot 10^3 \text{ kg} \cdot \text{m}^{-3}$. As noted by Lynn and Reid, the term “is the individual density gradient defined by vertical displacement of a water parcel (as opposed to the geometric density gradient). For discrete samples the density difference ($\delta \rho$) between two samples is taken after one is adiabatically displaced to the depth of the other.” For the results at any standard level (k), the computation was performed by displacing parcels at the next deeper standard level ($k+1$) to level k .

The actual procedure for using stability checks to flag sets of data points was as follows. To a depth of 30 m, stability (E) inversions in excess of $3 \cdot 10^{-2} \text{ kg} \cdot \text{m}^{-3}$ were flagged, and below this depth down to the 400 m level, inversions in excess of $2 \cdot 10^{-2} \text{ kg} \cdot \text{m}^{-3}$ were flagged. Below 400 m any inversion was flagged. To eliminate an inversion both temperature and salinity were flagged and eliminated from further use at both standard levels involved in the computation. In the actual processing a count was kept of the number of inversions in each cast. If a cast had two or more unacceptable inversions, as defined above, then the entire cast was eliminated from further use.

2.2.5. Subjective flagging of data

The temperature data were averaged by one-degree squares for input to the objective analysis program. After initial objective analyses were computed, the input set of one-degree means still contained questionable data contributing to unrealistic distributions, yielding intense bull's-eyes or spatial gradients. Examination of these features indicated that some of them were due to profiles from particular oceanographic cruises. In such cases, data from an entire cruise were flagged and withheld from further use by setting a flag on each profile from the cruise. In other cases, individual profiles or measurements

were found to cause these features and were flagged.

2.2.6. Representativeness of the data

Another quality control issue is data representativeness. The general paucity of data forces the compositing of all historical data to produce “climatological” fields. In a given one-degree square, there may be data from a month or season of one particular year, while in the same or a nearby square there may be data from an entirely different year. If there is large interannual variability in a region where scattered sampling in time has occurred, then one can expect the analysis to reflect this. Because the observations are scattered randomly with respect to time, except for a few limited areas, the results cannot, in a strict sense, be considered a true long-term climatological average.

For the present atlas we attempted to reduce the effects of irregular space-time sampling by the averaging of five “climatologies” computed for the following time periods: 1955-1964, 1965-1974, 1975-1984, 1985-1994, and 1995-2006. The first-guess field for each of these climatologies is the “all-data” monthly mean objectively analyzed temperature data.

We present smoothed analyses of historical means, based (in certain areas) on relatively few observations. We believe, however, that useful information about the oceans can be gained through our procedures and that the large-scale features are representative of the real ocean.

Basically, the data diminish in number with increasing depth. In the upper ocean, the all-data annual mean distributions are quite reasonable for defining large-scale features, but for the seasonal periods, the data base is inadequate in some regions. With respect to the deep ocean, in some areas the distribution of observations may be adequate

for some diagnostic computations but inadequate for other purposes. If an isolated deep basin or some region of the deep ocean has only one observation, then no horizontal gradient computations are meaningful. However, useful information is provided by the observation in the computation of other quantities (*e.g.*, a volumetric mean over a major ocean basin).

2.2.7. XBT drop rate error correction

It has been demonstrated that XBT temperature profiles made using T4, T6, and T7 probes exhibit a systematic error with depth that is associated with an incorrect drop rate equation for these instruments (Banes and Session, 1984; Hanawa *et al.*, 1994; Wright and Szabados, 1989; Singer, 1990; Hallock and Teague, 1992). The error in depth has a magnitude that equals approximately five percent of the actual depth. XBT instruments only measure temperature and time directly. The depth of an instrument is estimated from a manufacturer-supplied drop rate equation using the time elapsed after the probe enters the water. T4, T6, and T7 XBT probes, in fact, fall faster than the manufacturer’s specification. One manufacturer’s T5 XBTs have also recently been shown to have depth calculation errors (Kizu *et al.*, 2005).

A task team of the International Global Ocean Services System (IGOSS) of the Intergovernmental Oceanographic Commission (IOC) on “Quality Control for Automated Systems” has addressed the problem of how the international community should treat XBT data (IOC, 1992a; IOC, 1992b). One of their recommendations is that IGOSS continue using the existing drop-rate equations until international agreement is reached on a solution. It has been recommended that data centers continue to receive and distribute XBT data that are uncorrected for the systematic error. Some investigators have not followed this

guidance, and in other cases it is uncertain whether a correction was made or not before data being sent to an archive. Both these possibilities are indicated in our metadata for each profile. **We have made no correction to the depths of the observed level XBT profiles.** Thus, investigators, if they desire, can make whatever correction they need to the observed level data we are providing since we have not corrected these profiles for this error. However, in order to merge XBT data with other types of temperature measurements, and in order to produce climatologies and other analyses, by necessity we have corrected the drop-rate error in XBT profiles, as part of the process of interpolating the data to standard depth levels (the drop-rate correction was applied to the observed level data before interpolation to standard levels). **All T4, T6, and T7 XBT profiles and designated T5 XBT profiles that we have used in generating products at standard levels, or made available as part of our standard level profile data sets, have been corrected for the drop-rate error. If, in fact, users wish to use another procedure, but still use the XBT data set we have compiled, they can do so by applying their correction procedure to our observed level XBT profile data set, which has not been corrected for the drop-rate error, unless indicated by the metadata.**

The correction for XBT T4, T6, and T7 drop-rate error (Hanawa *et al.*, 1994) is:

$$z_c = 1.0417z_0 - 75.906 \cdot (1 - (102.063 \times 10^{-4} z_0)^{1/2})$$

in which z_0 is the originally calculated depth.

In addition to XBT depth corrections, Johnson (1995) has shown the necessity of depth correction for Sippican XCTDs, while Mizuno and Watanabe (1998) give depth corrections for TSK XCTDs. Both corrections follow the same procedure as for XBTs.

3. DATA PROCESSING PROCEDURES

3.1. Vertical interpolation to standard levels

Vertical interpolation of observed depth level data to standard depth levels followed procedures in JPOTS Editorial Panel (1991). These procedures are in part based on the work of Reiniger and Ross (1968). Four observed depth level values surrounding the standard depth level value were used, two values from above the standard level and two values from below the standard level. The pair of values furthest from the standard level are termed “exterior” points and the pair of values closest to the standard level are termed “interior” points. Paired parabolas were generated via Lagrangian interpolation. A reference curve was fitted to the four data points and used to define unacceptable interpolations caused by “overshooting” in the interpolation. When there were too few data points above or below the standard level to apply the Reiniger and Ross technique, we used a three-point Lagrangian interpolation. If three points were not available (either two above and one below or vice-versa), we used linear interpolation. In the event that an observation occurred exactly at the depth of a standard level, then a direct substitution was made. Table 3 provides the range of acceptable distances for which observed level data could be used for interpolation to a standard level.

3.2. Methods of analysis

3.2.1. Overview

An objective analysis scheme of the type described by Barnes (1964) was used to produce the fields shown in this atlas. This scheme had its origins in the work of Cressman (1959). In *World Ocean Atlas 1994* (WOA94), the Barnes (1973) scheme was used. This required only one “correction” to the first-guess field at each

grid point in comparison to the successive correction method of Cressman (1959) and Barnes (1964). This was to minimize computing time used in the processing. Barnes (1994) recommends a return to a multi-pass analysis when computing time is not an issue. Based on our own experience we agree with this assessment. The single pass analysis, used in WOA94, caused an artificial front in the Southeastern Pacific Ocean in a data sparse area (Anne Marie Treguier, personal communication). The analysis scheme used in generating WOA98, WOA01, WOA05, and WOA09 analyses uses a three-pass “correction” which does not result in the creation of this artificial front.

Inputs to the analysis scheme were one-degree square means of data values at standard levels (for time period and variable being analyzed), and a first-guess value for each square. For instance, one-degree square means for our “all-data” annual analysis were computed using all available data regardless of date of observation. For “all-data” July, we used all historical July data regardless of year of observation. For “decadal” July, we used July data only collected within a specified decade.

Analysis was the same for all standard depth levels. Each one-degree latitude-longitude square value was defined as being representative of its square. The 360x180 gridpoints are located at the intersection of half-degree lines of latitude and longitude. An influence radius was then specified. At those grid points where there was an observed mean value, the difference between the mean and the first-guess field was computed. Next, a correction to the first-guess value at all gridpoints was computed as a distance-weighted mean of all gridpoint difference values that lie within the area around the gridpoint defined by the influence radius. Mathematically, the

correction factor derived by Barnes (1964) is given by the expression:

$$C_{i,j} = \frac{\sum_{s=1}^n W_s Q_s}{\sum_{s=1}^n W_s} \quad (1)$$

in which:

(i,j) - coordinates of a gridpoint in the east-west and north-south directions respectively;

$C_{i,j}$ - the correction factor at gridpoint coordinates (i,j) ;

n - the number of observations that fall within the area around the point i,j defined by the influence radius;

Q_s - the difference between the observed mean and the first-guess at the S^{th} point in the influence area;

$$W_s = e^{-\frac{Er^2}{R^2}} \text{ (for } r \leq R; W_s = 0 \text{ for } r > R);$$

r - distance of the observation from the gridpoint;

R - influence radius;

$$E = 4.$$

The derivation of the weight function, W_s , will be presented in the following section. At each gridpoint we computed an analyzed value $G_{i,j}$ as the sum of the first-guess, $F_{i,j}$, and the correction $C_{i,j}$. The expression for this is

$$G_{i,j} = F_{i,j} + C_{i,j} \quad (2)$$

If there were no data points within the area defined by the influence radius, then the correction was zero, the first-guess field was left unchanged, and the analyzed value was simply the first-guess value. This correction procedure was applied at all gridpoints to produce an analyzed field. The resulting field was first smoothed with a median filter

(Tukey, 1974; Rabiner *et al.*, 1975) and then smoothed with a five-point smoother of the type described by Shuman (1957) (hereafter referred as five-point Shuman smoother). The choice of first-guess fields is important and we discuss our procedures in section 3.2.5.

The analysis scheme is set up so that the influence radius, and the number of five-point smoothing passes can be varied with each iteration. The strategy used is to begin the analysis with a large influence radius and decrease it with each iteration. This technique allows us to analyze progressively smaller scale phenomena with each iteration.

The analysis scheme is based on the work of several researchers analyzing meteorological data. Bergthorsson and Doos (1955) computed corrections to a first-guess field using various techniques: one assumed that the difference between a first-guess value and an analyzed value at a gridpoint was the same as the difference between an observation and a first-guess value at a nearby observing station. All the observed differences in an area surrounding the gridpoint were then averaged and added to the gridpoint first-guess value to produce an analyzed value. Cressman (1959) applied a distance-related weight function to each observation used in the correction in order to give more weight to observations that occur closest to the gridpoint. In addition, Cressman introduced the method of performing several iterations of the analysis scheme using the analysis produced in each iteration as the first-guess field for the next iteration. He also suggested starting the analysis with a relatively large influence radius and decreasing it with successive iterations so as to analyze smaller scale phenomena with each pass.

Sasaki (1960) introduced a weight function that was specifically related to the density of observations, and Barnes (1964, 1973)

extended the work of Sasaki. The weight function of Barnes (1964) has been used here. The objective analysis scheme we used is in common use by the mesoscale meteorological community. Several studies of objective analysis techniques have been made. Achtemeier (1987) examined the “concept of varying influence radii for a successive corrections objective analysis scheme.” Seaman (1983) compared the “objective analysis accuracies of statistical interpolation and successive correction schemes.” Smith and Leslie (1984) performed an “error determination of a successive correction type objective analysis scheme.” Smith *et al.* (1986) made “a comparison of errors in objectively analyzed fields for uniform and non-uniform station distribution.”

3.2.2. Derivation of Barnes (1964) weight function

The principle upon which the Barnes (1964) weight function is derived is that “the two-dimensional distribution of an atmospheric variable can be represented by the summation of an infinite number of independent harmonic waves, that is, by a Fourier integral representation.” If $f(x,y)$ is the variable, then in polar coordinates (r,θ) , a smoothed or filtered function $g(x,y)$ can be defined:

$$g(x, y) = \frac{1}{2\pi} \int_0^{2\pi} \int_0^\infty \eta f(x + r \cos \theta, y + r \sin \theta) d\left(\frac{r^2}{4K}\right) d\theta \quad (3)$$

in which r is the radial distance from a gridpoint whose coordinates are (x,y) . The weight function is defined as

$$\eta = e^{-\frac{r^2}{4K}} \quad (4)$$

which resembles the Gaussian distribution. The shape of the weight function is determined by the value of K , which relates

to the distribution of data. The determination of K follows. The weight function has the property that

$$\frac{1}{2\pi} \int_0^{2\pi} \int_0^{\infty} \eta d \left(\frac{r^2}{4K} \right) d\theta = 1 \quad (5)$$

This property is desirable because in the continuous case (3) the application of the weight function to the distribution $f(x,y)$ will not change the mean of the distribution. However, in the discrete case (1), we only sum the contributions to within the distance R . This introduces an error in the evaluation of the filtered function, because the condition given by (5) does not apply. The error can be pre-determined and set to a reasonably small value in the following manner. If one carries out the integration in (5) with respect to θ , the remaining integral can be rewritten as

$$\int_0^R \eta d \left(\frac{r^2}{4K} \right) + \int_R^{\infty} \eta d \left(\frac{r^2}{4K} \right) = 1 \quad (6)$$

Defining the second integral as ε yields

$$\int_0^R e^{-\frac{r^2}{4K}} d \left(\frac{r^2}{4K} \right) = 1 - \varepsilon \quad (7)$$

Integrating (7), we obtain

$$\varepsilon = e^{-\frac{R^2}{4K}} \quad (7a)$$

Taking the natural logarithm of both sides of (7a) leads to an expression for K ,

$$K = R^2 / 4E \quad (7b)$$

where $E \equiv -\ln \varepsilon$.

Rewriting (4) using (7b) leads to the form of weight function used in the evaluation of (1).

Thus, choice of E and the specification of R determine the shape of the weight function.

Levitus (1982) chose $E = 4$ which corresponds to a value of ε of approximately

0.02. This choice implies with respect to (7) the representation of more than 98 percent of the influence of any data around the gridpoint in the area defined by the influence radius R .

This analysis (WOA09) and previous analyses (WOA94, WOA98, WOA01, and WOA05) used $E = 4$.

Barnes (1964) proposed using this scheme in an iterative fashion similar to Cressman (1959). Levitus (1982) used a four-iteration scheme with a variable influence radius for each pass. WOA94 used a one-iteration scheme. WOA98, WOA01, WOA05, and WOA09 employed a three-iteration scheme with a variable influence radius.

3.2.3. Derivation of Barnes (1964) response function

It is desirable to know the response of a data set to the interpolation procedure applied to it. Following Barnes (1964) and reducing to one-dimensional case we let

$$f(x) = A \sin(\alpha x) \quad (8)$$

in which $\alpha = 2\pi/\lambda$ with λ being the wavelength of a particular Fourier component, and substitute this function into equation (3) along with the expression for η in equation (4). Then

$$g(x) = D[A \sin(\alpha x)] = Df(x) \quad (9)$$

in which D is the response function for one application of the analysis and defined as

$$D = e^{-\left(\frac{\alpha R}{4}\right)^2} = e^{-\left(\frac{\pi R}{2\lambda}\right)^2}$$

The phase of each Fourier component is not changed by the interpolation procedure. The results of an analysis pass are used as the first-guess for the next analysis pass in an iterative fashion. The relationship between the filtered function $g(x)$ and the response function after N iterations as derived by Barnes (1964) is

$$g_N(x) = f(x)D \sum_{n=1}^N (1-D)^{n-1} \quad (10)$$

Equation (10) differs trivially from that given by Barnes. The difference is due to our first-guess field being defined as a zonal average, annual mean, seasonal mean, or monthly mean for “all-data” climatologies, whereas Barnes used the first application of the analysis as a first-guess. “All-data” monthly climatologies were used as first-guess fields for each “decadal” monthly climatologies. Barnes (1964) also showed that applying the analysis scheme in an iterative fashion will result in convergence of the analyzed field to the observed data field. However, it is not desirable to approach the observed data too closely, because at least seven or eight gridpoints are needed to represent a Fourier component.

The response function given in (10) is useful in two ways: it is informative to know what Fourier components make up the analyses, and the computer programs used in generating the analyses can be checked for correctness by comparison with (10).

3.2.4. Choice of response function

The distribution of temperature observations (see appendices) at different depths and for the different averaging periods, are not regular in space or time. At one extreme, regions exist in which every one-degree square contains data and no interpolation needs to be performed. At the other extreme are regions in which few if any data exist. Thus, with variable data spacing the average separation distance between gridpoints containing data is a function of geographical position and averaging period. However, if we computed and used a different average separation distance for each variable at each depth and each averaging period, we would be generating analyses in which the wavelengths of observed phenomena might differ from one depth level to another and

from one season to another. In WOA94, a fixed influence radius of 555 kilometers was used to allow uniformity in the analysis of all variables. For the present analyses (as well as for WOA98 and WOA01), a three-pass analysis, based on Barnes (1964), with influence radii of 888, 666, and 444 km was used.

Inspection of (1) shows that the difference between the analyzed field and the first-guess field values at any gridpoint is proportional to the sum of the weighted-differences between the observed mean and first-guess at all gridpoints containing data within the influence area.

The reason for using the five-point Shuman smoother and the median smoother is that our data are not evenly distributed in space. As the analysis moves from regions containing data to regions devoid of data, small-scale discontinuities may develop. The five-point Shuman and median smoothers are used to eliminate these discontinuities. The five-point Shuman smoother does not affect the phase of the Fourier components that comprise an analyzed field.

The response function for the analyses presented in these atlases are given in Table 4 and Figure 1. For comparison purposes, the response function used by Levitus (1982), WOA94, and others are also presented. The response function represents the smoothing inherent in the objective analysis described above plus the effects of one application of the five-point Shuman smoother and one application of a five-point median smoother. The effect of varying the amount of smoothing in North Atlantic sea surface temperature (SST) fields has been quantified by Levitus (1982) for a particular case. In a region of strong SST gradient such as the Gulf Stream, the effect of smoothing can easily be responsible for differences between analyses exceeding 1.0°C.

To avoid the problem of the influence region extending across land or sills to adjacent basins, the objective analysis routine employs basin “identifiers” to preclude the use of data from adjacent basins. Table 5 lists these basins and the depth at which no exchange of information between basins is allowed during the objective analysis of data, *i.e.*, “depths of mutual exclusion.” Some regions are nearly, but not completely, isolated topographically. Because some of these nearly isolated basins have water mass properties that are different from surrounding basins, we have chosen to treat these as isolated basins as well. Not all such basins have been identified because of the complicated structure of the sea floor. In Table 5, a region marked with an “*” can interact with adjacent basins except for special areas such as the Isthmus of Panama.

3.2.5. First-guess field determination

There are gaps in the data coverage and, in some parts of the world ocean, there exist adjacent basins whose water mass properties are individually nearly homogeneous but have distinct basin-to basin differences. Spurious features can be created when an influence area extends over two basins of this nature (basins are listed in Table 5). Our choice of first-guess field attempts to minimize the creation of such features. To provide a first-guess field for the annual analysis at any standard level, we first zonally averaged the observed temperature data in each one-degree latitude belt by individual ocean basins. The annual analysis was then used as the first-guess for each seasonal analysis and each seasonal analysis was used as a first-guess for the appropriate monthly analysis if computed.

We then reanalyzed the temperature data using the newly produced analyses as first-guess fields described as follows and as shown in Figure 2. A new annual mean was computed as the mean of the twelve monthly

analyses for the upper 1500 m, and the mean of the four seasons below 1500 m depth. This new annual mean was used as the first-guess field for new seasonal analyses. These new seasonal analyses in turn were used to produce new monthly analyses. This procedure produces slightly smoother means.

These monthly mean objectively analyzed temperature fields were used as the first-guess fields for each “decadal” monthly climatology.

More importantly we recognize that fairly large data-void regions exist, in some cases to such an extent that a seasonal or monthly analysis in these regions is not meaningful. Geographic distribution of observations for the all-data annual periods (see appendices) is excellent for upper layers of the ocean. By using an all-data annual mean, first-guess field regions where data exists for only one season or month will show no contribution to the annual cycle. By contrast, if we used a zonal average for each season or month, then, in those latitudes where gaps exist, the first-guess field would be heavily biased by the few data points that exist. If these were anomalous data in some way, an entire basin-wide belt might be affected.

One advantage of producing “global” fields for a particular compositing period (even though some regions are data void) is that such analyses can be modified by investigators for use in modeling studies.

3.3. Choice of objective analysis procedures

Optimum interpolation (Gandin, 1963) has been used by some investigators to objectively analyze oceanographic data. We recognize the power of this technique but have not used it to produce analyzed fields. As described by Gandin (1963), optimum interpolation is used to analyze synoptic data

using statistics based on historical data. In particular, second-order statistics such as correlation functions are used to estimate the distribution of first order parameters such as means. We attempt to map most fields in this atlas based on relatively sparse data sets. Because of the paucity of data, we prefer not to use an analysis scheme that is based on second order statistics. In addition, as Gandin has noted, there are two limiting cases associated with optimum interpolation. The first is when a data distribution is dense. In this case, the choice of interpolation scheme makes little difference. The second case is when data are sparse. In this case, an analysis scheme based on second order statistics is of questionable value. For additional information on objective analysis procedures see Thiebaut and Pedder (1987) and Daley (1991).

3.4. Choice of spatial grid

The analyses that comprise WOA09 have been computed using the ETOPO5 land-sea topography to define ocean depths at each gridpoint (ETOPO5, 1988). From the ETOPO5 land mask, a quarter-degree land mask was created based on ocean bottom depth and land criteria. If four or more 5-minute square values out of a possible nine in a one-quarter-degree box were defined as land, then the quarter-degree gridbox was defined to be land. If no more than two of the 5-minute squares had the same depth value in a quarter-degree box, then the average value of the 5-minute ocean depths in that box was defined to be the depth of the quarter-degree gridbox. If three or more 5-minute squares out of the nine had a common bottom depth, then the depth of the quarter-degree box was set to the most common depth value. The same method was used to go from a quarter-degree to a one-degree resolution. In the one-degree resolution case, at least four points out of a possible sixteen (in a one-degree square) had

to be land in order for the one-degree square to remain land and three out of sixteen had to have the same depth for the ocean depth to be set. These criteria yielded a mask that was then modified by:

- a) Connecting the Isthmus of Panama,
- b) Maintaining an opening in the Straits of Gibraltar and in the English Channel,
- c) Connecting the Kamchatka Peninsula and the Baja Peninsula to their respective continents.

The quarter-degree mask was created as an intermediate step to ensure consistency between the present work and future high-resolution analysis of temperature and salinity.

3.5. Stabilization of Temperature and Salinity Climatologies

Temperature and salinity climatologies are calculated separately. There are many more temperature data than salinity data. Even when there are salinity measurements, there are not always concurrent temperature measurements. As a result, when density is calculated from standard level climatologies of temperature and salinity, instabilities may result in the vertical density field. (Stability is defined in section 2.4.4.) While instabilities do occur in the ocean on an instantaneous time frame, these instabilities are usually short-lived and not characteristic of the mean density field. Appendices A (Section 8.1) and B (Section 8.2) describe a method we have employed to minimally alter climatological temperature and salinity profiles to achieve a stable water column everywhere in the world ocean. The method is based on the method of Jackett and McDougall (1995). The final temperature and salinity climatologies reflect the alterations due to this process.

4. RESULTS

The appendices in this atlas include three types of horizontal maps in black and white as a function of selected standard depth levels for temperature:

- a) Number of temperature observations in each one-degree latitude-longitude grid used in the objective analysis binned into 1 to 5 and greater than 5 numbers of observations. Each map includes the total number of observations.
- b) Objectively analyzed temperature fields. One-degree grids for which there were less than three values available in the objective analysis defined by the influence radius are denoted by a “+” symbol.
- c) Seasonal and monthly temperature difference fields from the annual mean field. One-degree grids for which there were less than three values available in the objective analysis defined by the influence radius are denoted by a “+” symbol.

The maps are arranged by composite time periods: annual, seasonal, month. The table of contents includes a list of all figures included in the appendices. We note that the complete set of all climatological maps (in color), objectively analyzed fields and associated statistical fields at all standard depth levels shown in Table 1 are available on DVD by sending an e-mail request to NODC.Services@noaa.gov and on-line at www.nodc.noaa.gov/OC5/indprod.html. The complete set of maps, data fields, and documentation are available on-line at www.nodc.noaa.gov/OC5/indprod.html and on DVD. Table 6 describes all available temperature maps and data fields.

All of the figures in the appendices use consistent symbols and notations for displaying information. Continents are displayed as solid black areas. Oceanic areas

shallower than the standard depth level being displayed are displayed as solid light gray areas. The objectively analyzed distribution fields include the minimum and maximum observed values as well as the nominal contour interval used. In addition, these maps may include in some cases additional contour lines displayed as dashed black lines. All of the maps were computer drafted using Generic Mapping Tools (Wessel and Smith, 1998).

We describe next the computation of annual and seasonal fields (section 4.1) and available objective and statistical fields (section 4.2).

4.1. Computation of annual and seasonal fields

After completion of all of our analyses we define a final annual analysis as the average of our twelve monthly mean fields in the upper 1500 m of the ocean. Below 1500 m depth we define an annual analysis as the mean of the four seasonal analyses. Our final seasonal analyses are defined as the average of the monthly analyses in the upper 1500 m of the ocean. Monthly fields were computed as the average of five “decadal” monthly analyses.

4.2. Available statistical fields

Table 6 lists all objective and statistical fields calculated as part of WOA09. Climatologies of temperature and associated statistics described in this document, as well as global figures of same can be obtained both on-line at www.nodc.noaa.gov/OC5/WOA09/pr_woa09.html and on DVD by sending a request to NODC.Services@noaa.gov.

The sample standard deviation in a gridbox was computed using:

$$s = \sqrt{\frac{\sum_{n=1}^N (x_n - \bar{x})^2}{N-1}} \quad (11)$$

in which x_n = the n^{th} data value in the gridbox, \bar{x} = mean of all data values in the gridbox, and N = total number of data values in the gridbox. The standard error of the mean was computed by dividing the standard deviation by the square root of the number of observations in each gridbox.

In addition to statistical fields, the land/ocean bottom mask and basin definition mask are also available on the above mentioned website. A user could take the standard depth level data from WOD09 with flags and these masks, and recreate the WOA09 fields following the procedures outlined in this document. Explanations and data formats for the data files are found under documentation on the WOA09 webpage.

4.3. Obtaining WOA09 fields online

The objective and statistical data fields can be obtained online in different digital formats at the WOA09 webpage (http://www.nodc.noaa.gov/OC5/WOA09/pr_woa09.html) and on DVD by sending a request to NODC.Services@noaa.gov. The WOA09 fields can be obtained in ASCII format (WOA native and comma separated value [CSV]) and netCDF through our WOA09 web page. For users interested in specific geographic areas, the World Ocean Atlas Select (WOAselect) selection tool can be used to designate a subset geographic area, depth, and oceanographic variable to view and optionally download climatological means or related statistics in shapefile format which is compatible with GIS software such as ArcMap. WOA09 includes a digital collection of "JPEG" and high resolution graphic (PDF) images of the objective and statistical fields. In addition,

WOA09 can be obtained in Ocean Data View (ODV) format (<http://odv.awi.de/>). WOA09 will be available through other online locations as well. WOA98, WOA01, and WOA05 are presently served through the IRI/LDEO Climate Data Library with access to statistical and objectively analyzed fields in a variety of digital formats (<http://iridl.ldeo.columbia.edu/>).

5. SUMMARY

In the preceding sections we have described the results of a project to objectively analyze all historical ocean temperature data in WOD09. We desire to build a set of climatological analyses that are identical in all respects for all variables including relatively data sparse variables such as nutrients. This provides investigators with a consistent set of analyses to work with.

One advantage of the analysis techniques used in this atlas is that we know the amount of smoothing by objective analyses as given by the response function in Table 4 and Figure 1. We believe this to be an important function for constructing and describing a climatology of any geophysical parameter. Particularly when computing anomalies from a standard climatology, it is important that the synoptic field be smoothed to the same extent as the climatology, to prevent generation of spurious anomalies simply through differences in smoothing. A second reason is that purely diagnostic computations require a minimum of seven or eight gridpoints to represent any Fourier component with accuracy. Higher order derivatives will require more smoothing.

We have attempted to create objectively analyzed fields and data sets that can be used as a "black box." We emphasize that some quality control procedures used are subjective. For those users who wish to make their own choices, all the data used in

our analyses are available both at standard depth levels as well as observed depth levels (www.nodc.noaa.gov/OC5/WOD09/pr_wod09.html). The results presented in this atlas show some features that are suspect and may be due to non-representative data that were not flagged by the quality control techniques used. Although we have attempted to eliminate as many of these features as possible by flagging the data which generate these features, some obviously could remain. Some may eventually turn out not to be artifacts but rather to represent real features, not yet capable of being described in a meaningful way due to lack of data.

6. FUTURE WORK

Our analyses will be updated when justified by additional observations. As more data are received at NODC/WDC, we will also be able to produce improved higher resolution climatologies for temperature.

7. REFERENCES

- Achtemeier, G. L., 1987. On the concept of varying influence radii for a successive corrections objective analysis. *Mon. Wea. Rev.*, 11, 1761-1771.
- Antonov, J. I., S. Levitus, T. P. Boyer, M. E. Conkright, T. D. O' Brien, and C. Stephens, 1998a. *World Ocean Atlas 1998. Vol. 1: Temperature of the Atlantic Ocean*. NOAA Atlas NESDIS 27, U.S. Gov. Printing Office, Washington, D.C., 166 pp.
- Antonov, J. I., S. Levitus, T. P. Boyer, M. E. Conkright, T. D. O' Brien, and C. Stephens, 1998b. *World Ocean Atlas 1998. Vol. 2: Temperature of the Pacific Ocean*. NOAA Atlas NESDIS 28, U.S. Gov. Printing Office, Washington, D.C., 166 pp.

- Antonov, J. I., S. Levitus, T. P. Boyer, M. E. Conkright, T. D. O' Brien, C. Stephens, and B. Trotsenko, 1998c. *World Ocean Atlas 1998. Vol. 3: Temperature of the Indian Ocean*. NOAA Atlas NESDIS 29, U.S. Gov. Printing Office, Washington, D.C., 166 pp.
- Antonov, J. I., R. A. Locarnini, T. P. Boyer, H. E. Garcia, and A. V. Mishonov, 2006. *World Ocean Atlas 2005, Vol. 2: Salinity*. S. Levitus, Ed., NOAA Atlas NESDIS 62, U.S. Gov. Printing Office, Washington, D.C. 182 pp.
- Antonov, J. I., D. Seidov, T. P. Boyer, R. A. Locarnini, A. V. Mishonov, and H. E. Garcia, 2010. *World Ocean Atlas 2009, Volume 2: Salinity*. S. Levitus, Ed., NOAA Atlas NESDIS 69, U.S. Gov. Printing Office, Washington, D.C. 184 pp.
- Banes, J. and M. H. Sessions, 1984: A field performance test of the Sippican deep aircraft-deployed expendable bathythermograph. *J. Geophys. Res.*, 89, 3615-3621.
- Barnes, S. L., 1964. A technique for maximizing details in numerical weather map analysis. *J. App. Meteor.*, 3, 396-409.
- Barnes, S. L., 1973. Mesoscale objective map analysis using weighted time series observations. *NOAA Technical Memorandum ERL NSSL-62*, 60 pp.
- Barnes, S. L., 1994. Applications of the Barnes Objective Analysis Scheme, Part III: Tuning for Minimum Error. *J. Atmos. Oceanic Technol.*, 11, 1459-1479.
- Bergthorsson, P. and B. Doos, 1955. Numerical Weather map analysis. *Tellus*, 7, 329-340.

- Boyer, T. P. and S. Levitus, 1994. Quality control and processing of historical temperature, salinity and oxygen data. *NOAA Technical Report NESDIS 81*, 65 pp.
- Boyer, T. P., S. Levitus, J. I. Antonov, M. E. Conkright, T. D. O' Brien, and C. Stephens, 1998a. *World Ocean Atlas 1998 Vol. 4: Salinity of the Atlantic Ocean*. NOAA Atlas NESDIS 30, U.S. Gov. Printing Office, Washington, D.C., 166 pp.
- Boyer, T. P., S. Levitus, J. I. Antonov, M. E. Conkright, T. D. O' Brien, and C. Stephens, 1998b. *World Ocean Atlas 1998 Vol. 5: Salinity of the Pacific Ocean*. NOAA Atlas NESDIS 31, U.S. Gov. Printing Office, Washington, D.C., 166 pp.
- Boyer, T. P., S. Levitus, J. I. Antonov, M. E. Conkright, T. D. O' Brien, and C. Stephens, B. Trotsenko, 1998c. *World Ocean Atlas 1998 Vol. 6: Salinity of the Indian Ocean*. NOAA Atlas NESDIS 32, U.S. Gov. Printing Office, Washington, D.C., 166 pp.
- Boyer, T. P., C. Stephens, J. I. Antonov, M. E. Conkright, R. A. Locarnini, T. D. O'Brien, and H. E. Garcia, 2002. *World Ocean Atlas 2001, Vol. 2: Salinity*. S. Levitus, Ed., NOAA Atlas NESDIS 50, U.S. Government Printing Office, Washington, D.C., 165 pp.
- Boyer, T. P., S. Levitus, H. E. Garcia, R. A. Locarnini, C. Stephens, and J. I. Antonov, 2004. Objective Analyses of Annual, Seasonal, and Monthly Temperature and Salinity for the World Ocean on a $\frac{1}{4}$ degree Grid. *International Journal of Climatology*, 25, 931-945.
- Boyer, T. P., J. I. Antonov, O. K. Baranova, H. E. Garcia, D. R. Johnson, R. A. Locarnini, A. V. Mishonov, T. D. O'Brien, D. Seidov, I. V. Smolyar, and M. M. Zweng, 2009. *World Ocean Database 2009*. S. Levitus, Ed., NOAA Atlas NESDIS 66, U.S. Gov. Printing Office, Washington, D.C., 219 pp., DVDs.
- Conkright, M. E., S. Levitus, and T. P. Boyer, 1994. *World Ocean Atlas 1994, Vol. 1: Nutrients*. NOAA Atlas NESDIS 1, U.S. Gov. Printing Office, Washington, D.C., 150 pp.
- Conkright, M. E., T. D. O' Brien, S. Levitus, T. P. Boyer, J. I. Antonov, and C. Stephens, 1998a. *World Ocean Atlas 1998 Vol. 10: Nutrients and Chlorophyll of the Atlantic Ocean*. NOAA Atlas NESDIS 36, U.S. Gov. Printing Office, Washington, D.C., 245 pp.
- Conkright, M. E., T. D. O' Brien, S. Levitus, T. P. Boyer, J. I. Antonov, and C. Stephens, 1998b. *World Ocean Atlas 1998 Vol. 11: Nutrients and Chlorophyll of the Pacific Ocean*. NOAA Atlas NESDIS 37, U.S. Gov. Printing Office, Washington, D.C., 245 pp.
- Conkright, M. E., T. D. O' Brien, S. Levitus, T. P. Boyer, J. I. Antonov, and C. Stephens, 1998c. *World Ocean Atlas 1998 Vol. 12: Nutrients and Chlorophyll of the Indian Ocean*. NOAA Atlas NESDIS 38, U.S. Gov. Printing Office, Washington, D.C., 245 pp.
- Conkright, M. E., H. E. Garcia, T. D. O'Brien, R. A. Locarnini, T. P. Boyer, C. Stephens, and J. I. Antonov, 2002. *World Ocean Atlas 2001, Vol. 4: Nutrients*. S. Levitus, Ed., NOAA Atlas NESDIS 52, U.S. Government Printing Office, Washington, D.C., 392 pp.
- Cressman, G. P., 1959. An operational objective analysis scheme. *Mon. Wea. Rev.*, 87, 329-340.

- Daley, R., 1991. *Atmospheric Data Analysis*. Cambridge University Press, Cambridge, 457 pp.
- ETOPO5, 1988. Data Announcements 88-MGG-02, Digital relief of the Surface of the Earth. NOAA, National Geophysical Data Center, Boulder, CO.
- Gandin, L. S., 1963. *Objective Analysis of Meteorological fields*. Gidrometeorol Izdat, Leningrad (translation by Israel program for Scientific Translations, Jerusalem, 1966, 242 pp).
- Garcia, H. E., R. A. Locarnini, T. P. Boyer, and J. I. Antonov, 2006a. *World Ocean Atlas 2005, Vol. 3: Dissolved Oxygen, Apparent Oxygen Utilization, and Oxygen Saturation*. S. Levitus, Ed., NOAA Atlas NESDIS 63, U.S. Government Printing Office, Washington, D.C., 342 pp.
- Garcia H. E., R. A. Locarnini, T. P. Boyer, and J. I. Antonov, 2006b. *World Ocean Atlas 2005: Vol. 4: Nutrients (phosphate, nitrate, silicate)*, S. Levitus, Ed., NOAA Atlas NESDIS 64, U.S. Gov. Printing Office, Washington, D.C., 396 pp.
- Garcia, H. E., R. A. Locarnini, T. P. Boyer, and J. I. Antonov, 2010a. *World Ocean Atlas 2009, Volume 3: Dissolved Oxygen, Apparent Oxygen Utilization, and Oxygen Saturation*. S. Levitus, Ed., NOAA Atlas NESDIS 70, U.S. Government Printing Office, Washington, D.C., 344 pp.
- Garcia, H. E., R. A. Locarnini, T. P. Boyer, and J. I. Antonov, 2010b. *World Ocean Atlas 2009, Volume 4: Nutrients (phosphate, nitrate, silicate)*. S. Levitus, Ed., NOAA Atlas NESDIS 71, U.S. Government Printing Office, Washington, D.C., 398 pp.
- Hallock, Z. R. and W. J. Teague, 1992. The fall rate of the T-7 XBT. *J. Atmos. Oceanic Technol.*, 9, 470-483.
- Hanawa, K., P. Raul, R. Bailey, A. Sy, and M. Szabados, 1994. Calculation of new depth equations for expendable bathythermographs using a temperature-error-free method (application to Sippican/TSK T-7, T-6 and T-4 XBTs). *IOC Technical Series*, 42, 46 pp.
- Hesselberg, T. and H. U. Sverdrup, 1914. Die Stabilitätsverhältnisse des Seewassers bei Vertikalen Verschiebungen. *Aarb. Bergen Mus.*, No. 14, 17 pp.
- IOC, 1992a. Summary report of the IGOSS task team on quality control for automated systems and addendum to the summary report. *IOC/INF-888*, 1992.
- IOC, 1992b. Summary report of the IGOSS task team on quality control for automated systems and addendum to the summary report. *IOC/INF-888-append.*, 1992.
- IOC, 1998. *Global Temperature-Salinity Profile Programme (GTSP) – Overview and Future*. IOC Technical Series, 49, Intergovernmental Oceanographic Commission, Paris, 12 pp.
- Jackett, D. R. and T. J. McDougall, 1995. Minimal Adjustment of Hydrographic Profiles to Achieve Static Stability. *J. Atmos. Oceanic Technol.*, 12, 381-389.
- JPOTS (Joint Panel on Oceanographic Tables and Standards) Editorial Panel, 1991. Processing of Oceanographic Station Data. UNESCO, Paris, 138 pp.
- Johnson, D. R., T. P. Boyer, H. E. Garcia, R. A. Locarnini, O. K. Baranova, and M. M. Zweng, 2009. *World Ocean Database 2009 Documentation*. Ed.

- Sydney Levitus. NODC Internal Report 20, U.S. Government Printing Office, Washington, D.C., 175 pp.
- Johnson G. C., 1995. Revised XCTD fall-rate equation coefficients from CTD data. *J. Atmos. Oceanic Technol.*, 12, 1367-1373.
- Kizu, S., H. Yoritaka, and K. Hanawa, 2005: A new fall-rate equation for T-5 Expendable Bathythermograph (XBT) by TSK. *J. Oceanogr.*, 61, 115-121.
- Levitus, S., 1982. *Climatological Atlas of the World Ocean*, NOAA Professional Paper No. 13, U.S. Gov. Printing Office, 173 pp.
- Levitus, S. and T. P. Boyer, 1994a. *World Ocean Atlas 1994, Vol. 2: Oxygen*. NOAA Atlas NESDIS 2, U.S. Gov. Printing Office, Washington, D.C., 186 pp.
- Levitus, S. and T. P. Boyer, 1994b. *World Ocean Atlas 1994, Vol. 4: Temperature*. NOAA Atlas NESDIS 4, U.S. Gov. Printing Office, Washington, D.C., 117 pp.
- Levitus, S. and G. Isayev, 1992. A polynomial approximation to the International Equation of State for Seawater. *J. Atmos. Oceanic Technol.*, 9, 705-708.
- Levitus, S., R. Burgett, and T. P. Boyer, 1994. *World Ocean Atlas 1994, Vol. 3: Salinity*. NOAA Atlas NESDIS 3, U.S. Gov. Printing Office, Washington, D.C., 99 pp.
- Levitus, S., S. Sato, C. Maillard, N. Mikhailov, P. Caldwell, and H. Dooley, 2005, *Building Ocean Profile-Plankton Databases for Climate and Ecosystem Research*, NOAA Technical Report NESDIS 117, U.S. Government Printing Office, Washington, D.C., 29 pp.
- Locarnini, R. A., T. D. O'Brien, H. E. Garcia, J. I. Antonov, T. P. Boyer, M. E. Conkright, and C. Stephens, 2002. *World Ocean Atlas 2001, Vol. 3: Oxygen*. S. Levitus, Ed., NOAA Atlas NESDIS 51, U.S. Government Printing Office, Washington, D.C., 286 pp.
- Locarnini, R. A., A. V. Mishonov, J. I. Antonov, T. P. Boyer, and H. E. Garcia, 2006. *World Ocean Atlas 2005, Vol. 1: Temperature*. S. Levitus, Ed., NOAA Atlas NESDIS 61, U.S. Government Printing Office, Washington, D.C. 182 pp.
- Lynn, R. G. and J. L. Reid, 1968. Characteristics and circulation of deep and abyssal waters. *Deep-Sea Res.*, 15, 577-598.
- Mizuno, K. and T. Watanabe, 1998. Preliminary results of in-situ XCTD/CTD comparison test. *J. Oceanogr.*, 54(4), 373-380.
- Neumann, G. and W. J. Pierson, 1966: *Principles of Physical Oceanography*. Prentice Hall Inc., Englewood Cliffs, N.J., 545 pp.
- O' Brien, T. D., S. Levitus, T. P. Boyer, M. E. Conkright, J. I. Antonov, and C. Stephens, 1998a. *World Ocean Atlas 1998 Vol. 7: Oxygen of the Atlantic Ocean*. NOAA Atlas NESDIS 33, U.S. Gov. Printing Office, Washington, D.C., 234 pp.
- O' Brien, T. D., S. Levitus, T. P. Boyer, M. E. Conkright, J. I. Antonov, and C. Stephens, 1998b. *World Ocean Atlas 1998 Vol. 8: Oxygen of the Pacific Ocean*. NOAA Atlas NESDIS 34, U.S. Gov. Printing Office, Washington, D.C., 234 pp.
- O' Brien, T. D., S. Levitus, T. P. Boyer, M. E. Conkright, J. I. Antonov, and C. Stephens, 1998c. *World Ocean Atlas*

- 1998 Vol. 9: *Oxygen of the Indian Ocean*. NOAA Atlas NESDIS 35, U.S. Gov. Printing Office, Washington, D.C., 234 pp.
- Rabiner, L. R., M. R. Sambur, and C. E. Schmidt, 1975. Applications of a nonlinear smoothing algorithm to speech processing, *IEEE Trans. on Acoustics, Speech and Signal Processing*, 23, 552-557.
- Reiniger, R. F. and C. F. Ross, 1968. A method of interpolation with application to oceanographic data. *Deep-Sea Res.*, 9, 185-193.
- Sasaki, Y., 1960. An objective analysis for determining initial conditions for the primitive equations. Ref. 60-1 6T, Atmospheric Research Lab., Univ. of Oklahoma Research Institute, Norman, 23 pp.
- Seaman, R. S., 1983. Objective Analysis accuracies of statistical interpolation and successive correction schemes. *Australian Meteor. Mag.*, 31, 225-240.
- Shuman, F. G., 1957. Numerical methods in weather prediction: II. Smoothing and filtering. *Mon. Wea. Rev.*, 85, 357-361.
- Singer, J. J., 1990. On the error observed in electronically digitized T-7 XBT data. *J. Atmos. Oceanic Technol.*, 7, 603-611.
- Smith, D. R., and F. Leslie, 1984. Error determination of a successive correction type objective analysis scheme. *J. Atmos. Oceanic Technol.*, 1, 121-130.
- Smith, D. R., M. E. Pumphry, and J. T. Snow, 1986. A comparison of errors in objectively analyzed fields for uniform and nonuniform station distribution, *J. Atmos. Oceanic Technol.*, 3, 84-97.
- Stephens, C., J. I. Antonov, T. P. Boyer, M. E. Conkright, R. A. Locarnini, T. D. O'Brien, and H. E. Garcia, 2002. *World Ocean Atlas 2001, Vol. 1: Temperature*. S. Levitus, Ed., NOAA Atlas NESDIS 49, U.S. Government Printing Office, Washington, D.C., 167 pp.
- Sverdrup, H. U., M. W. Johnson, and R. H. Fleming, 1942. *The Oceans: Their physics, chemistry, and general biology*. Prentice Hall, 1060 pp.
- Thiebaux, H. J. and M. A. Pedder, 1987. *Spatial Objective Analysis: with applications in atmospheric science*. Academic Press, 299 pp.
- Tukey, J. W., 1974. Nonlinear (nonsuperposable) methods for smoothing data, in "Cong. Rec.", 1974 EASCON, 673 pp.
- Wessel, P. and W. H. F. Smith, 1998. New, improved version of Generic Mapping Tools released, *EOS Trans. Amer. Geophys. U.*, 79, 579.
- Wright, D. and M. Szabados, 1989. Field evaluation of real-time XBT systems. *Oceans 89 Proc.*, 5, 1621-1626.

Table 1. Descriptions of climatologies for temperature. The standard depth levels are shown in Table 3.

OCEANOGRAPHIC VARIABLE	DEPTHS FOR ANNUAL CLIMATOLOGY	DEPTHS FOR SEASONAL CLIMATOLOGY	DEPTHS FOR MONTHLY CLIMATOLOGY	DATASETS USED TO CALCULATE CLIMATOLOGY
Temperature	0-5500 meters (33 levels)	0-5500 meters (33 levels)	0-1500 meters (24 levels)	OSD, CTD, MRB, PFL, DRB, UOR, SUR, XBT, MBT, GLD

Table 2. Descriptions of datasets in WOD09 used to calculate the temperature climatologies.

OSD	BOTTLE (REVERSING THERMOMETERS), LOW-RESOLUTION CONDUCTIVITY-TEMPERATURE-DEPTH (CTD), LOW-RESOLUTION XCTD DATA, AND PLANKTON DATA
CTD	High-Resolution Conductivity-Temperature-Depth (CTD) data and High-Resolution XCTD data
MBT	Mechanical Bathythermograph (MBT) data, DBT, micro-BT
XBT	Expendable Bathythermograph (XBT) data
SUR	Surface only data (bucket, thermosalinograph)
MRB	Moored buoy data from TAO (Tropical Atmosphere-Ocean), PIRATA (Pilot Research Moored Array in the Tropical Atlantic), MARNET, RAMA (Research Moored Array for African-Asian-Australian Monsoon Analysis and Prediction), and TRITON (Japan-JAMSTEC)
PFL	Profiling float data
DRB	Drifting buoy data from surface drifting buoys with thermistor chains
UOR	Undulating Oceanographic Recorder data from a Conductivity-Temperature-Depth (CTD) probe mounted on a towed undulating vehicle
GLD	Glider data

Table 3. Acceptable distances (m) for defining interior and exterior values used in the Reiniger-Ross scheme for interpolating observed level data to standard levels.

Standard Level number	Standard depths (m)	Acceptable distances (m) for interior values	Acceptable distances (m) for exterior values
1	0	5	200
2	10	50	200
3	20	50	200
4	30	50	200
5	50	50	200
6	75	50	200
7	100	50	200
8	125	50	200
9	150	50	200
10	200	50	200
11	250	100	200
12	300	100	200
13	400	100	200
14	500	100	400
15	600	100	400
16	700	100	400
17	800	100	400
18	900	200	400
19	1000	200	400
20	1100	200	400
21	1200	200	400
22	1300	200	1000
23	1400	200	1000
24	1500	200	1000
25	1750	200	1000
26	2000	1000	1000
27	2500	1000	1000
28	3000	1000	1000
29	3500	1000	1000
30	4000	1000	1000
31	4500	1000	1000
32	5000	1000	1000
33	5500	1000	1000

Table 4. Response function of the objective analysis scheme as a function of wavelength for WOA09 and earlier analyses. Response function is normalized to 1.0.

Wavelength*	Levitus (1982)	WOA94	WOA98, 01, 05, 09
360ΔX	1.000	0.999	1.000
180ΔX	1.000	0.997	0.999
120ΔX	1.000	0.994	0.999
90ΔX	1.000	0.989	0.998
72ΔX	1.000	0.983	0.997
60ΔX	1.000	0.976	0.995
45ΔX	1.000	0.957	0.992
40ΔX	0.999	0.946	0.990
36ΔX	0.999	0.934	0.987
30ΔX	0.996	0.907	0.981
24ΔX	0.983	0.857	0.969
20ΔX	0.955	0.801	0.952
18ΔX	0.923	0.759	0.937
15ΔX	0.828	0.671	0.898
12ΔX	0.626	0.532	0.813
10ΔX	0.417	0.397	0.698
9ΔX	0.299	0.315	0.611
8ΔX	0.186	0.226	0.500
6ΔX	3.75×10^{-2}	0.059	0.229
5ΔX	1.34×10^{-2}	0.019	0.105
4ΔX	1.32×10^{-3}	2.23×10^{-3}	2.75×10^{-2}
3ΔX	2.51×10^{-3}	1.90×10^{-4}	5.41×10^{-3}
2ΔX	5.61×10^{-7}	5.30×10^{-7}	1.36×10^{-6}

For $\Delta X = 111$ km, the meridional separation at the Equator.

Table 5. Basins defined for objective analysis and the shallowest standard depth level for which each basin is defined.

#	BASIN	STANDARD DEPTH LEVEL	#	BASIN	STANDARD DEPTH LEVEL
1	Atlantic Ocean	1*	30	North American Basin	29
2	Pacific Ocean	1*	31	West European Basin	29
3	Indian Ocean	1*	32	Southeast Indian Basin	29
4	Mediterranean Sea	1*	33	Coral Sea	29
5	Baltic Sea	1	34	East Indian Basin	29
6	Black Sea	1	35	Central Indian Basin	29
7	Red Sea	1	36	Southwest Atlantic Basin	29
8	Persian Gulf	1	37	Southeast Atlantic Basin	29
9	Hudson Bay	1	38	Southeast Pacific Basin	29
10	Southern Ocean	1*	39	Guatemala Basin	29
11	Arctic Ocean	1	40	East Caroline Basin	30
12	Sea of Japan	1	41	Marianas Basin	30
13	Kara Sea	8	42	Philippine Sea	30
14	Sulu Sea	10	43	Arabian Sea	30
15	Baffin Bay	14	44	Chile Basin	30
16	East Mediterranean	16	45	Somali Basin	30
17	West Mediterranean	19	46	Mascarene Basin	30
18	Sea of Okhotsk	19	47	Crozet Basin	30
19	Banda Sea	23	48	Guinea Basin	30
20	Caribbean Sea	23	49	Brazil Basin	31
21	Andaman Basin	25	50	Argentine Basin	31
22	North Caribbean	26	51	Tasman Sea	30
23	Gulf of Mexico	26	52	Atlantic Indian Basin	31
24	Beaufort Sea	28	53	Caspian Sea	1
25	South China Sea	28	54	Sulu Sea II	14
26	Barents Sea	28	55	Venezuela Basin	14
27	Celebes Sea	25	56	Bay of Bengal	1*
28	Aleutian Basin	28	57	Java Sea	6
29	Fiji Basin	29	58	East Indian Atlantic Basin	32

Basins marked with a “” can interact with adjacent basins in the objective analysis.

Table 6. Objective and statistical data fields calculated as part of WOA09
 (√ denotes field was calculated and is publicly available).

STATISTICAL FIELD	ONE-DEGREE FIELD CALCULATED	FIVE-DEGREE STATISTICS CALCULATED
Objectively analyzed climatology	√	
Statistical mean	√	√
Number of observations	√	√
Seasonal (monthly) climatology minus annual climatology	√	
Standard deviation from statistical mean	√	√
Standard error of the statistical mean	√	√
Statistical mean minus objectively analyzed climatology	√	
Number of mean values within radius of influence	√	

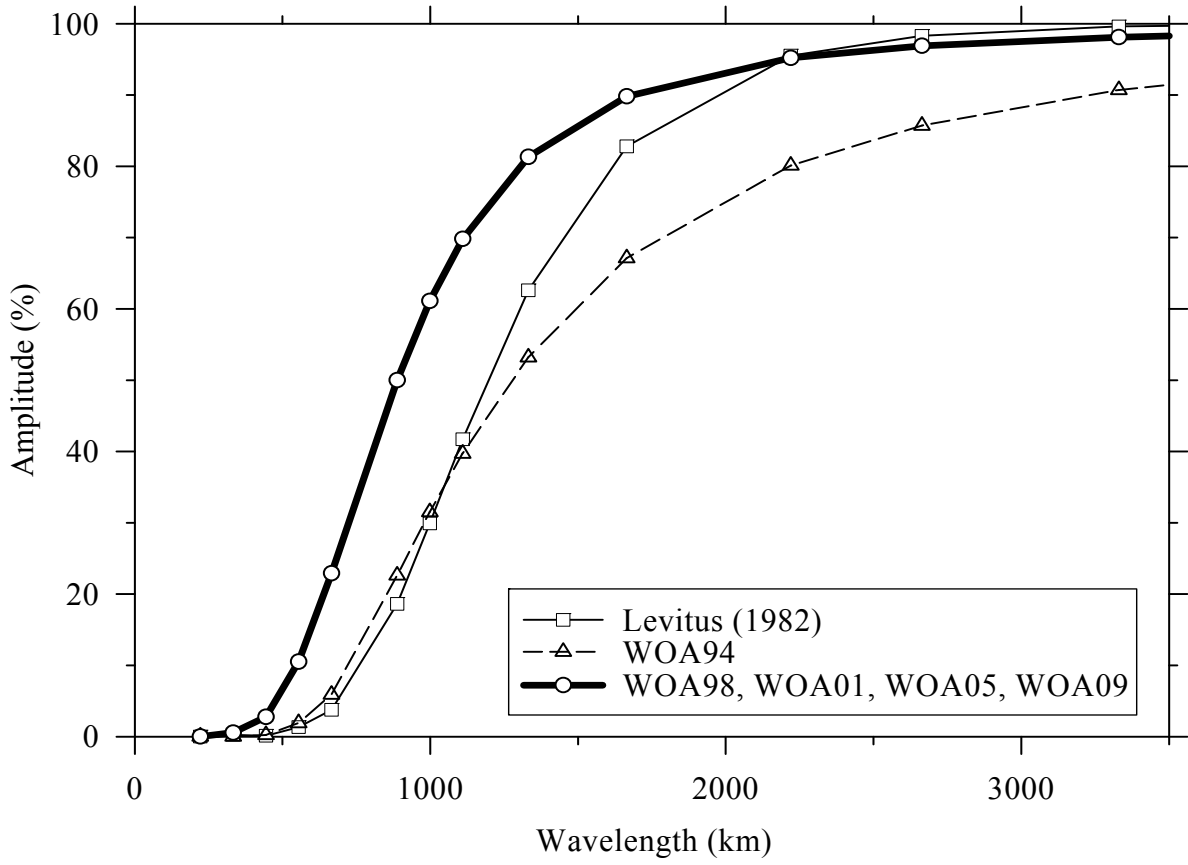


Figure 1. Response function of the WOA09, WOA05, WOA01, WOA98, WOA94, and Levitus (1982) objective analysis schemes.

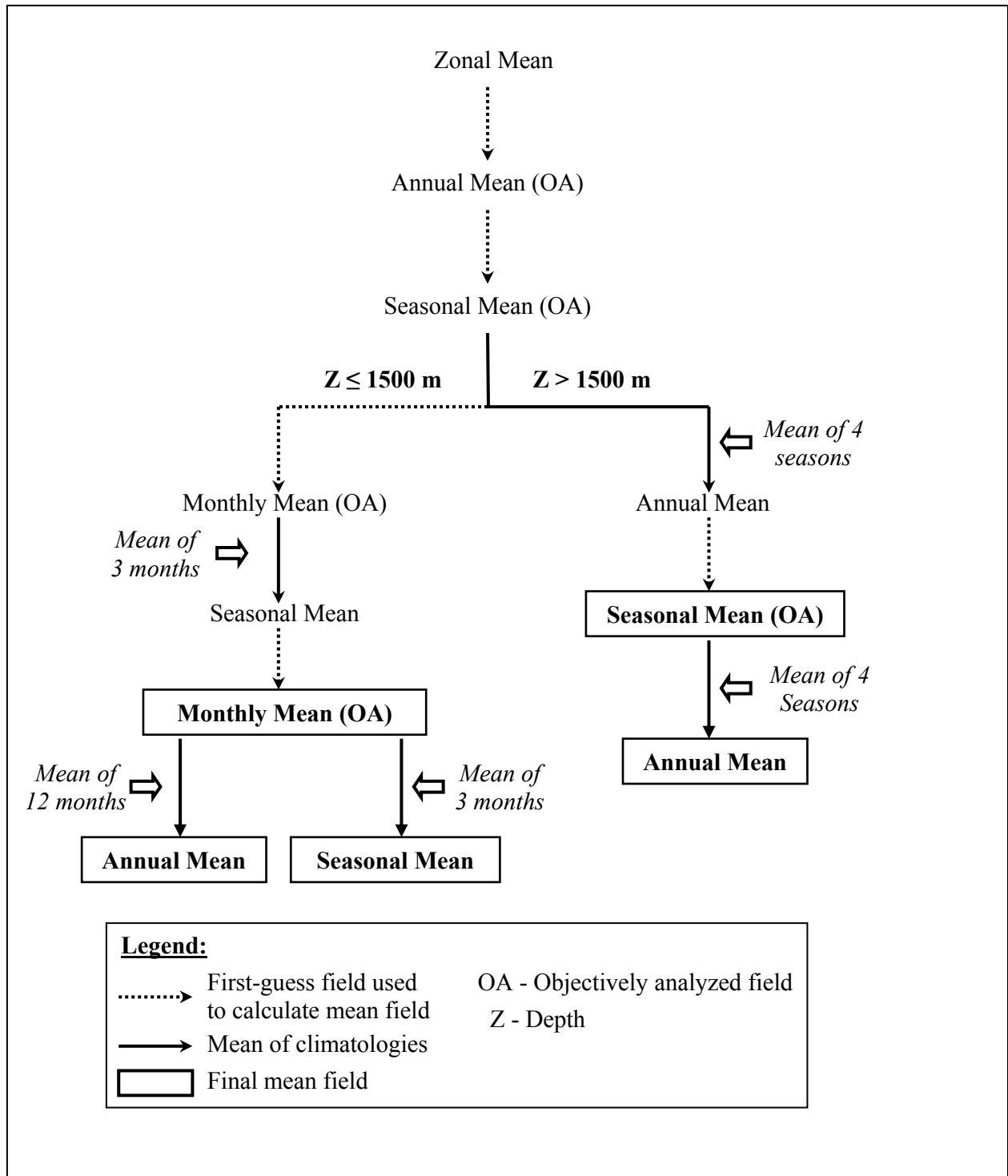


Figure 2. Scheme used in computing annual, seasonal, and monthly objectively analyzed means for temperature. The final monthly, seasonal, and annual climatologies were density stabilized – see section 3.5.

8. APPENDICES

8.1. Appendix A: Stabilization of Temperature and Salinity Climatologies

A1. Defining and identifying instabilities

The first step is to identify the instabilities. The definition of stability is found in section 2.2.4. It will be repeated here for convenience. We use the Hesselberg-Sverdrup criteria described by Lynn and Reid (1968) and Neumann and Pierson (1966). The stability, \mathbf{E} , is defined as

$$\mathbf{E} = \lim_{\partial z \rightarrow 0} \frac{1}{\rho_0} \frac{\delta \rho}{\partial z}$$

in which

z = depth,

ρ = *in-situ* density,

$\rho_0 = 1.02 \cdot 10^3 \text{ kg} \cdot \text{m}^{-3}$, and

$\delta \rho$ = vertical density difference.

As noted by Lynn and Reid, the stability, \mathbf{E} , is “the individual density gradient defined by vertical displacement of a water parcel (as opposed to the geometric density gradient). For discrete samples, the density difference ($\delta \rho$) between two adjacent levels is taken after one is adiabatically displaced to the depth of the other.”

Computationally,

$$\mathbf{E} = \rho_a - \rho$$

in which

ρ_a = the local potential density, and

ρ = *in-situ* density.

Thus, this computational form for \mathbf{E} involves computing the local potential density of the deeper of the two adjacent levels with respect to the depth of the shallower of the two adjacent levels. If this density is lower than the *in-situ* density at the higher level, this represents an instability. The density (actually, the density anomaly) computation followed procedures in JPOTS Editorial Panel (1991). A profile of \mathbf{E} is generated from the profiles of objectively analyzed temperature and salinity for each one-degree grid box. There will be $\mathbf{N}-1$ values of \mathbf{E} in the profile, where \mathbf{N} corresponds to the number of depth levels at a given gridpoint.

If an instability is encountered between two levels, \mathbf{k} and $\mathbf{k}+1$, it must be determined whether to change the temperature and/or salinity to achieve stability, and whether to make the change on level \mathbf{k} or level $\mathbf{k}+1$. The goal is to change the original climatological profiles of temperature and salinity, and by extension, of density, as little as possible while achieving stability.

A2. Deciding to change temperature and or salinity

Before deciding which level to change, the values of $\Delta T/\Delta z$ and $\Delta S/\Delta z$, the gradients of temperature and salinity between adjacent levels involved in the instability, are examined. This helps determine if the temperature or salinity profile, or both, are to be changed to stabilize the density field. The values of $\Delta T/\Delta z$ and $\Delta S/\Delta z$ are in different units, but some judgments can be made looking at the sign of the values:

If $\Delta T/\Delta z > 0$, $\Delta S/\Delta z > 0$: only temperature is changed.

If $\Delta T/\Delta z < 0$, $\Delta S/\Delta z < 0$: only salinity is changed.

If $\Delta T/\Delta z > 0$, $\Delta S/\Delta z < 0$: local linear trend test employed as described in section A3.

Increasing temperature acts to decrease density (when temperature is above the temperature of the maximum density for the given salinity), decreasing salinity acts to decrease density. If temperature increases while salinity between levels is static or increasing, we assume it is the temperature gradient which is responsible for the instability between these two levels. Conversely, if the salinity is decreasing, while the temperature is static or decreasing, we assume it is the salinity data which are responsible for the noted instability. In the example in Appendix B, instabilities #1, #2.2, #2.3, #5, #6, and #6.1 are stabilized using the results of this gradient test.

If temperature is increasing while salinity is decreasing between levels, more information is necessary to understand to what extent temperature and salinity are involved in creating the given instability, as we describe in the next section.

A3. Local linear trend in density

A method we term the “local linear trend in density” is employed. This method is illustrated in instability #2 in the example in Appendix B. In this method, the levels $k-2$ to $k+3$ from the temperature and salinity profiles at the grid-point containing the instability are used, where k is the upper level involved in the density instability and $k+1$ is the deeper level. The change in density due to temperature (holding salinity constant) and the change in density due to salinity (holding temperature constant) are estimated for each set of adjacent levels [($k-2, k-1$), ($k-1, k$), ($k, k+1$), ($k+1, k+2$), ($k+2, k+3$)]. The constant values of temperature and salinity used are the average values of these parameters over their entire profiles at the grid-point containing the instability.

The density change due to temperature (salinity) between levels k and $k+1$ is used as a base value from which the density change due to temperature (salinity) between the other four sets of adjacent levels are subtracted:

$$\text{LLT}(T) = (\Delta\rho_k(T)/\Delta z)_{k,k+1} - (\Delta\rho_{k-2}(T)/\Delta z)_{k-2,k-1} - (\Delta\rho_{k-1}(T)/\Delta z)_{k-1,k} - (\Delta\rho_{k+1}(T)/\Delta z)_{k+1,k+2} - (\Delta\rho_{k+2}(T)/\Delta z)_{k+2,k+3}$$

$$\text{LLT}(S) = (\Delta\rho_k(S)/\Delta z)_{k,k+1} - (\Delta\rho_{k-2}(S)/\Delta z)_{k-2,k-1} - (\Delta\rho_{k-1}(S)/\Delta z)_{k-1,k} - (\Delta\rho_{k+1}(S)/\Delta z)_{k+1,k+2} - (\Delta\rho_{k+2}(S)/\Delta z)_{k+2,k+3}$$

This localized linear trend gives some sense of how the temperature and salinity are changing in the general vicinity of the instability in similar units, and how that change is affecting the density structure. For instance, if $(\Delta\rho_k(T)/\Delta z)_{k,k+1} < 0$ by only a small amount, and $(\Delta\rho_{k-2}(T)/\Delta z)_{k-2,k-1}$, $(\Delta\rho_{k-1}(T)/\Delta z)_{k-1,k}$, $(\Delta\rho_{k+1}(T)/\Delta z)_{k+1,k+2}$, and $(\Delta\rho_{k+2}(T)/\Delta z)_{k+2,k+3}$ are also < 0 , it would appear that

the temperature is naturally increasing in the vicinity of the instability and the value of $LLT(T)$ would reflect this by being positive, or only slightly negative. Conversely, if the base $(\Delta\rho_k(S)/\Delta z)_{k,k+1} < 0$, while $(\Delta\rho_{k-2}(S)/\Delta z)_{k-2,k-1}$, $(\Delta\rho_{k-1}(S)/\Delta z)_{k-1,k}$, $(\Delta\rho_{k+1}(S)/\Delta z)_{k+1,k+2}$, and $(\Delta\rho_{k+2}(S)/\Delta z)_{k+2,k+3}$ are all > 0 , this would indicate the possibility that $(\Delta\rho_k(S)/\Delta z)_{k,k+1}$ may be an anomaly, and the salinity may be the source of the instability. The resultant negative $LLT(S)$ makes this apparent.

Thus,

If $LLT(T) < 0$, $LLT(S) > 0$: only temperature changed

If $LLT(T) > 0$, $LLT(S) < 0$: only salinity changed.

If $LLT(T) < 0$, $LLT(S) < 0$ (or $LLT(T) > 0$, $LLT(S) > 0$) : the combined linear trend test is employed.

The combined linear trend test, which is employed in instabilities #4, #4.1, and #4.2 of the example in Appendix B, is as follows:

$$Tp = LLT(T)/(LLT(T)+LLT(S))*100$$

$$Sp = LLT(S)/(LLT(T)+LLT(S))*100$$

Where Tp is percent of change in density due to temperature and Sp is percent of change in density due to salinity

In this case, temperature and salinity are both changed. The change in salinity is responsible for Sp percent of the total change in density needed to achieve stability. The change in temperature is made to account for Tp percent of the total change in density needed to achieve stability.

A4. How temperature and salinity are changed

Once it is determined which variable to change, it is simple to make the change. If the upper level needs to be adjusted, the temperature is increased and/or the salinity is decreased to come as close as possible to $\rho_k(\mathbf{k}+1) - \rho_k(\mathbf{k}) = 0$. This is the minimum static stability. It is not always possible to reach zero exactly due to the precision limitations of the temperature and salinity values used. The distributed ASCII versions of the temperature and salinity climatologies has four digits to the right of the decimal. So, the maximum significant digits to the right of the decimal for density is also four. As a result, the minimum value for the quantity $\rho_k(\mathbf{k}+1) - \rho_k(\mathbf{k}) \leq |10^{-4}|$. If the lower level needs to be adjusted, the temperature at this level is decreased and/or salinity is increased to reach the minimum static stability. Deciding whether the upper or lower level should be changed is addressed in the next section. Since $\rho_k(\mathbf{k}+1)$ is calculated using potential temperature relative to the upper level, it is actually the potential temperature which meets the $\rho_k(\mathbf{k}+1) - \rho_k(\mathbf{k}) = 0$ requirement, and then from this, the *in situ* temperature is determined.

In the case where both the temperature and salinity are changed, temperature is changed first. If the upper level is being adjusted, the temperature which fits the density $\rho_k(\mathbf{k})'$, (where $\rho_k(\mathbf{k})' = \rho_k(\mathbf{k}) - ((\rho_k(\mathbf{k}+1) - \rho_k(\mathbf{k})) * (Tp/100))$) is calculated. That is, the temperature which changes the density of the upper level Tp percent of the total change in density which is necessary to achieves stability. This temperature is then used to calculate the salinity which achieves minimum static stability.

Similarly, if the lower level is changed, the temperature which fits the density $\rho_k(\mathbf{k}+1)' = \rho_k(\mathbf{k}+1) + ((\rho_k(\mathbf{k}+1) - \rho_k(\mathbf{k})) * (Tp/100))$ is calculated, and then the salinity which, coupled with this temperature approaches $\rho_k(\mathbf{k}+1)' - \rho_k(\mathbf{k})' = 0$, is found.

The temperature is calculated by adding or subtracting small increments to the original temperature until the desired density is approached as closely as possible. The salinity is approximated using the polynomial approximation to the International Equation of State (Levitus and Isayev, 1992) from the given density and temperature, and adding or subtracting small increments until the desired density is approached as closely as possible.

A5. Deciding on changing either upper or lower level

The temperature and/or salinity at only one level need to be changed to achieve static stability (all non-negative values in the **E** profile). The temperature/salinity change is made at the level which will least affect the overall profiles of temperature and salinity. Both the necessary change at the upper level (**k**) only and the change at the lower level (**k+1**) only are calculated. The possible new temperature and/or salinity values at the upper level (**k**) are used to calculate a new **E** value between the upper level (**k**) and the next higher (**k-1**) level (when possible) to see if a new instability is created. Likewise, a new **E** value between the lower level and the next lower level (**k+2**, when possible) is calculated from the proposed new temperature and/or salinity values. If there is a new instability created by changing the upper level, but no new instability created by changing the lower level, the lower level is the level where the temperature and/or salinity changes will be implemented, and vice-versa.

If there are new instabilities in both cases, successively higher levels are checked using the proposed temperature/salinity changes to the upper level involved in the instability, calculating **E** between the successively higher levels and the upper level with the temperature/salinity changes. The same is done between the lower level with its proposed temperature/salinity values and each successive lower level. This continues one step past either reaching the topmost level or the bottommost level. For instance, if there are nine levels in a profile, and the instability takes place between levels five and six, the proposed temperature/salinity changes to level five and to level six will be checked a maximum of four times for new instabilities. **E** will be calculated between the lower level and levels seven, eight, and nine, respectively. **E** will be recalculated between the upper level and levels four, three, two, and one. If there are instabilities all the way to the bottom, this would be equal to instabilities all the way up the water column, to level two. One more check on the upper levels is made, and if this too is an instability, this will be deemed as the upper level proposed temperature/salinity changes creating more instabilities than the lower level proposed temperature/salinity changes, and the temperature and salinities changes to the lower level will be implemented. This test was implemented in all cases in Appendix B, except instabilities #2.1 and #5.

If no new instabilities are created, or if the same number of new instabilities are created in both the upper level proposed temperature/salinity changes and the lower level proposed temperature/salinity changes, the smallest necessary change is preferred.

Let $|dt(\mathbf{k})|$ = temperature adjustment to level **k** (absolute value of the difference between original temperature value and adjusted temperature value.)

$|ds(\mathbf{k})|$ = salinity adjustment to level \mathbf{k} (absolute value of the difference between original salinity value and adjusted salinity value.)

If $|dt(\mathbf{k})| < |dt(\mathbf{k}+1)|$ and $|ds(\mathbf{k})| < |ds(\mathbf{k}+1)|$: change \mathbf{k} (upper level)

If $|dt(\mathbf{k})| > |dt(\mathbf{k}+1)|$ and $|ds(\mathbf{k})| > |ds(\mathbf{k}+1)|$: change $\mathbf{k}+1$ (lower level)

If $|dt(\mathbf{k})| > |dt(\mathbf{k}+1)|$ and $|ds(\mathbf{k})| < |ds(\mathbf{k}+1)|$ or

$|dt(\mathbf{k})| < |dt(\mathbf{k}+1)|$ and $|ds(\mathbf{k})| > |ds(\mathbf{k}+1)|$: use adjusted linear trend test

The above test was implemented in examples #2.2 and #5 in Appendix B, but only for the trivial case in which only temperature was changed.

The adjusted linear trend (which is not demonstrated in Appendix B) is as follows:

The local linear trend in density is computed for temperature and salinity for the case of the change to the upper level (\mathbf{k}) and the case of the change to the lower level ($\mathbf{k}+1$). Then the complete adjusted linear, LLTA, is

$$LLTA(\mathbf{k}) = \text{abs}[(LLT(T(\mathbf{k})+dt(\mathbf{k}))) + LLT(S(\mathbf{k})+ds(\mathbf{k}))] - (LLT(T(\mathbf{k}))+LLT(S(\mathbf{k})))$$

If $LLTA(\mathbf{k}) < LLTA(\mathbf{k}+1)$: change \mathbf{k} (upper level)

If $LLTA(\mathbf{k}) \geq LLTA(\mathbf{k}+1)$: change $\mathbf{k}+1$ (lower level)

In other words, the level that is changed is the level which minimizes total change to local linear trends of density with respects to temperature and salinity. In the case where the change is equal, the choice of level to change is ambiguous and the level changed is arbitrarily set to the lower level.

A6. Finalizing temperature and salinity profiles

Each **E** profile is checked for instabilities starting at the surface and then proceeding to the bottom, or the thirty-third standard level (5500 meters), whichever is reached first. If an instability is encountered, it is dealt with as detailed above. If this process results in a new instability involving the upper layer involved in the old instability and the level above that one, this new instability is dealt with before proceeding further down the profile. This process is continued until there are no instabilities in the entire **E** profile. It may be that the temperature and salinity at a level are changed numerous times in the process of stabilizing the entire **E** profile. This may be necessary to achieve the minimum possible changes over the entire temperature and salinity profiles while still creating stability.

Then the procedure is performed again on the original **E** profile, this time starting from the bottom of the profile and continuing to the surface. There are grid boxes which have large gradients in temperature and/or salinity near the surface. If these large gradients are involved in an instability, and the **E** profile is being checked from the top down, these large gradients may propagate changes down to lower depths when they should be confined to the upper depths. When the profile is checked from the bottom up, the lower depths are usually preserved intact while changes are made only in the upper layer.

Finally, the density change due to temperature and to salinity is calculated for the top- down and the bottom-up cases. The density change from the original profile due to temperature is calculated at each level, as is the density change from the original profile due to salinity.

The density changes at each level are added together and divided by the number of levels minus one to get an average density change for both the top-down case and the bottom-up case. The case with the lowest average density change is the case implemented. If average density change is equal in both cases, the top down case is implemented.

8.2. Appendix B: Example of Stabilization

The area chosen for this example is the one-degree latitude-longitude box centered at 53.5°S - 171.5°E from a previous version of the World Ocean Atlas (1998, WOA98). This is on the New Zealand Plateau, with a bottom depth below 1000 meters and above 1100 meters. The month is October, during the early austral summer. There is a deep mixed layer in this area, using vertical temperature change as an indicator. There is no temperature or salinity data within the chosen one-degree box. Thus the objectively analyzed values in this one-degree box will be dependent on the seasonal objectively analyzed field and the data in near-by one-degree grid boxes. There is much more temperature data than salinity data on the New Zealand plateau for October. This contributes to six small (on the order of 10^{-2} $\text{kg}\cdot\text{m}^{-3}$) inversions in the local potential density field calculated from objectively analyzed temperature and salinity fields. The whole numbers in bold below correspond to the numbered instability shown in Table B1 and Table B2. The decimal numbers in bold shown in Table B2 correspond to new instabilities created while correcting the original instabilities. Table B2 shows the final, stabilized profiles.

#1 Working first from the bottom of the profile upwards, the first inversion is encountered between 400 and 500 meters depth. The temperature rises with the increase in depth here, from 6.8275°C to 7.4001°C, while the salinity increases from 34.2852 PSS to 34.3123 PSS. Using the criteria of the gradient test, the temperature will be changed here, while the salinity will not. Now it remains to decide whether to change the temperature value at 400 m or 500 m. If the temperature value at 400 m is changed to eliminate the instability, a new instability will be created between 300 m and 400 m depth. No new instability is created if the value at 500 m depth is changed. Therefore the temperature value at 500 m depth is changed to 6.9838°C to create a situation where the stability is within 10^{-4} $\text{kg}\cdot\text{m}^{-3}$ of neutral stability.

#2 Continuing upwards, the next instability is found between 250 and 300 m depth. The temperature here rises from 7.0962°C to 7.1622°C. The salinity decreases from 34.3415 PSS to 34.3367 PSS. The gradient test can not be used in this case, since both temperature and salinity are acting to decrease stability. The next test, the local linear trend in density must be implemented. This test ascertains the general tendency of the temperature and salinity in the immediate area of the instability. Is the temperature generally increasing? Is the salinity generally increasing? In this case, the levels to be checked, listed by depths are:

k-2 = 150 m depth, $t(\mathbf{k-2}) = 6.8919^\circ\text{C}$, $s(\mathbf{k-2}) = 34.3697$ PSS (instability)

k-1 = 200 m depth, $t(\mathbf{k-1}) = 6.9363^\circ\text{C}$, $s(\mathbf{k-1}) = 34.3364$ PSS (instability)

k = 250 m depth, $t(\mathbf{k}) = 7.0962^\circ\text{C}$, $s(\mathbf{k}) = 34.3415$ PSS (instability)

$k+1$ = 300 m depth, $t(k+1) = 7.1622^{\circ}\text{C}$, $s(k+1) = 34.3367$ PSS

$k+2$ = 400 m depth, $t(k+2) = 6.8275^{\circ}\text{C}$, $s(k+2) = 34.2852$ PSS

$k+3$ = 500 m depth, $t(k+3) = 6.9838^{\circ}\text{C}$, $s(k+3) = 34.3123$ PSS

It is already known that the changes in both temperature and salinity between k and $k+1$ work to decrease stability, otherwise, this test would not be needed. Therefore the density change between levels k and $k+1$ keeping salinity constant is negative. The test is to see how large is the density change between levels k and $k+1$ in relation to the cumulative density changes between other adjacent levels, keeping salinity constant. The density changes between levels $k-2$ and $k-1$, and between levels $k-1$ and k are not used in this test for this case because the density structure between these adjacent levels are unstable and therefore assumed to include anomalous temperature and/or salinity values. The density change due only to temperature between levels $k+1$ and $k+2$ is positive and fairly large in comparison with the instability between k and $k+1$. The density change between levels $k+2$ and $k+3$ is negative. However, the cumulative valid density changes due only to temperature between adjacent levels in the immediate area of the instability between levels k and $k+1$ is positive and slightly larger in comparison with the absolute value of the instability between levels k and $k+1$. To get a numerical value for this comparison, the cumulative value of valid density changes due to temperature between adjacent levels in the immediate area of the instability between levels k and $k+1$ is subtracted from the value of the density change between levels k and $k+1$. If the result is positive, this denotes that the gradient of the temperature in the immediate area of the instability is of the same sign as the temperature gradient between levels k and $k+1$. This reinforces the idea that the temperature gradient between levels k and $k+1$ is probably not an anomaly, but follows the true pattern of the temperature profile. If the result is negative, this denotes that the temperature gradient between levels k and $k+1$ does not follow the pattern of adjacent areas of the temperature profile and is probably an anomaly.

Looking at the change in density between adjacent levels due to salinity, the change between levels $k+1$ and $k+2$ is quite large in comparison to the density change due to salinity between the levels k and $k+1$, where the instability occurs. The change between levels $k+2$ and $k+3$ in density due to salinity is negative and smaller in absolute value than the increase between levels $k+1$ and $k+2$.

The results for the local linear trend test in density for temperature and salinity are negative and positive respectively. These results lead to a change in temperature in either level k or level $k+1$ to rectify the instability. This is not the optimal trial for the local linear trend in density test because two of the four adjacent level density changes could not be used due to their own instabilities. If either the upper (k) value for temperature or lower ($k+1$) value is changed, new instabilities will result in the profile. In the case where instabilities already exist, (the upper level temperature value changed) the instabilities are exacerbated. But more levels will be affected if the upper level temperature value is changed. So the lower level ($k+1$) temperature value is changed to eliminate the instability between levels k and $k+1$. The new value at 300 m depth for temperature is 7.0748°C .

#2.1, #2.2 Because of this change, there is now an instability between 300 and 400 m depth. The gradient test reveals negative gradients in temperature and salinity. This leads to a new salinity value of 34.2894 PSS (from an old value of 34.2852 PSS) at 400 m depth. Temperature is unchanged. This causes a new instability between 400 and 500 m depth. The gradient test

indicates a change only to temperature. Since neither a change to the upper level or lower level will cause new instabilities, a temperature change to the lower level is implemented because it incurs a smaller change to the temperature at that level than would the change to the upper level. The new temperature value at 500 m depth is 6.9604°C (old value 6.9838°C).

#3 Since no new instabilities were created in the last change, checking proceeds up the profiles again. The next instability occurs between 200 and 250 m depth. The result of the gradient test and choosing the minimum change to the original values, is to change the temperature only, at 200 m depth, from 6.9363°C to 7.0628°C.

#4 The instability between 150 and 200 m depth cannot be resolved using the gradient test. The following levels are set for the local linear trend in density test:

k-2 = 100 m depth,	$t(\mathbf{k-2}) = 6.9753^\circ\text{C}$,	$s(\mathbf{k-2}) = 34.3280$ PSS
k-1 = 125 m depth,	$t(\mathbf{k-1}) = 6.9218^\circ\text{C}$,	$s(\mathbf{k-1}) = 34.3604$ PSS
k = 150 m depth,	$t(\mathbf{k}) = 6.8919^\circ\text{C}$,	$s(\mathbf{k}) = 34.3697$ PSS (instability)
k+1 = 200 m depth,	$t(\mathbf{k+1}) = 7.0628^\circ\text{C}$,	$s(\mathbf{k+1}) = 34.3364$ PSS
k+2 = 250 m depth,	$t(\mathbf{k+2}) = 7.0962^\circ\text{C}$,	$s(\mathbf{k+2}) = 34.3415$ PSS
k+3 = 300 m depth,	$t(\mathbf{k+3}) = 7.0748^\circ\text{C}$,	$s(\mathbf{k+3}) = 34.3367$ PSS.

Since this is an iterative process, the values for temperature at 250 and 300 m depth are the newly calculated values, not the original values.

In this case, the density with respects to temperature increases between levels **k-2** and **k-1**, between **k-1** and **k**, and between **k+2** and **k+3**. This is not completely offset by the decrease in density due to temperature between levels **k+1** and **k+2**. So the numerical value for temperature for the local linear trend in density is negative. For density with respects salinity, the value is positive for all adjacent levels except between **k+2** and **k+3**. The local linear trend in density for salinity is also negative. So this test is also inconclusive.

When this point is reached, both temperature and salinity will be changed. The extent to which they will be changed depends on their relative local linear trends in density. This is the reason for computing the local trends of temperature and salinity in like units. The local linear trend in density for temperature is $-0.0357 \text{ kg}\cdot\text{m}^{-3}$. The local linear trend in density for salinity is $-0.0592 \text{ kg}\cdot\text{m}^{-3}$. Using their ratio, 62% of the change in density necessary for stabilization will be accounted for by changing the salinity, 38% will be accounted for by changing the temperature. Changes on the upper level are found to cause fewer new instabilities than changes to the bottom level. The new values for 150 m depth are 7.0242°C for temperature and 34.3301 PSS for salinity.

#4.1 A new instability is created between 125 and 150 m depth. Again, both the gradient test and the local linear trend in density are inconclusive. Both temperature and salinity are changed, with salinity accounting for 75% of the change in density. The values at 125 m depth are changed from 6.9218°C to 6.9897°C for temperature and 34.3604 PSS to 34.3243 PSS for salinity.

#4.2 A new instability between 100 and 125 m depth is again resolved only by changing both temperature and salinity at 100 m. The new values are 6.9796°C and 34.3228 PSS for the

respective variables (old values 6.9753°C and 34.3280 PSS).

#5, #6, #6.1 The final two original instabilities, between 50 and 75 m depth and between 10 and 20 m depth are both resolved by the gradient test. The level of the change for the former instability is chosen on the basis of least change to the temperature, since no new instabilities are created. In this case the value of temperature at 50 m depth is changed from 6.9686°C to 7.0132°C. For the later case, the value of salinity at 10 m depth is changed from 34.4278 PSS to 34.3063 PSS. This creates one last instability between the surface and 10 m depth. The gradient test yields a change in the surface salinity from 34.4243 PSS to 34.3096 PSS. The level at which the change is made is based on the change which creates the fewest new instabilities.

A complete, altered, stable set of temperature and salinity profiles has now been achieved.

The entire process is repeated starting from the top and proceeding downwards through the profile. The changes to density at each level are calculated for the results of the top-down and bottom-up calculations. The procedure which cumulatively changes the original density structure least is chosen as the final result. The reason for doing both top-down and bottom-up procedures is that when there is a large instability near the surface, doing the top-down procedure can significantly alter the entire profile set, whereas bottom-up will confine the changes to the near surface portion. The converse is also true. So both procedures are performed to identify the procedure which changes the original the least.

The chosen profile is an extreme example of the stabilization process, used to illustrate all aspects of the procedure. Each instability is initially treated separately, and a single level in a profile may be altered many times due to changes in the surrounding levels before a fully stable set of temperature and salinity profiles is produced.

Table B1. Gridbox 171.5°E, 53.5°S improved WOA98 profiles before stabilization.¹

k	Depth (m)	Temperature (°C)	Salinity	ρ (kg·m⁻³)	ρ_a (kg·m⁻³)	E (kg·m⁻³)	Change #
1	0.0	7.1667	34.4243	26.9423	26.9476	0.0054	
2	10.0	7.1489	34.4278	26.9939	26.8982	-0.0957	#6
3	20.0	7.0465	34.2880	26.9443	26.9529	0.0085	
4	30.0	7.0050	34.2914	26.9990	27.0104	0.0114	
5	50.0	6.9686	34.2991	27.1028	27.0967	-0.0061	#5
6	75.0	7.0604	34.3073	27.2120	27.2406	0.0286	
7	100.0	6.9753	34.3280	27.3560	27.3892	0.0332	
8	125.0	6.9218	34.3604	27.5046	27.5164	0.0117	
9	150.0	6.8919	34.3697	27.6316	27.6000	-0.0316	#4
10	200.0	6.9363	34.3364	27.8302	27.8123	-0.0179	#3
11	250.0	7.0962	34.3415	28.0421	28.0295	-0.0126	#2
12	300.0	7.1622	34.3367	28.2593	28.2684	0.0092	
13	400.0	6.8275	34.2852	28.7281	28.6664	-0.0618	#1
14	500.0	7.4001	34.3123	29.1238	29.3699	0.2461	
15	600.0	6.2133	34.4022	29.8292	29.9386	0.1094	
16	700.0	5.9186	34.4868	30.3978	30.5869	0.1891	
17	800.0	4.5426	34.4904	31.0488	31.0754	0.0266	
18	900.0	4.1263	34.4558	31.5377	31.6539	0.1162	
19	1000.0	3.3112	34.4755	32.1176			

¹ The value of $\rho(\mathbf{k})$ was computed using values of temperature, salinity and pressure on standard depth level \mathbf{k} ; the value of $\rho_a(\mathbf{k})$ was computed using values of temperature and salinity on standard depth level $\mathbf{k}+1$ and pressure on standard depth level \mathbf{k} .

Table B2. Gridbox 171.5°E, 53.5°S improved WOA98 profiles after stabilization.²

k	Depth (m)	Temperature (°C)	Salinity	ρ (kg·m⁻³)	ρ_a (kg·m⁻³)	E(kg·m⁻³)	Change #
1	0.0	7.1667	34.3096	26.8519	26.8521	0.0002	#6.1
2	10.0	7.1489	34.3063	26.8982	26.8982	0.0000	#6
3	20.0	7.0465	34.2880	26.9443	26.9529	0.0085	
4	30.0	7.0050	34.2914	26.9990	27.0042	0.0051	
5	50.0	7.0132	34.2991	27.0967	27.0967	0.0000	#5
6	75.0	7.0604	34.3073	27.2120	27.2361	0.0240	
7	100.0	6.9796	34.3228	27.3513	27.3513	0.0000	#4.2
8	125.0	6.9897	34.3243	27.4667	27.4667	0.0000	#4.1
9	150.0	7.0242	34.3301	27.5820	27.5820	0.0000	#4
10	200.0	7.0628	34.3364	27.8123	27.8123	0.0000	#3
11	250.0	7.0962	34.3415	28.0421	28.0422	0.0000	#2
12	300.0	7.0748	34.3367	28.2719	28.2719	0.0001	#2.1
13	400.0	6.8275	34.2894	28.7314	28.7314	0.0000	#1, #2.2
14	500.0	6.9604	34.3123	29.1899	29.3699	0.1799	
15	600.0	6.2133	34.4022	29.8292	29.9386	0.1094	
16	700.0	5.9186	34.4868	30.3978	30.5869	0.1891	
17	800.0	4.5426	34.4904	31.0488	31.0754	0.0266	
18	900.0	4.1263	34.4558	31.5377	31.6539	0.1162	
19	1000.0	3.3112	34.4755	32.1176			

² The value of $\rho(\mathbf{k})$ was computed using values of temperature, salinity and pressure on standard depth level \mathbf{k} ; the value of $\rho_a(\mathbf{k})$ was computed using values of temperature and salinity on standard depth level $\mathbf{k}+1$ and pressure on standard depth level \mathbf{k} .

8.3. Appendix C: Maps of data distribution and climatological mean temperature for the annual compositing period for selected standard depth levels.

8.4. Appendix D: Maps of data distribution, climatological mean temperature, and difference from annual mean for each seasonal compositing period for selected standard depth levels.

8.5. Appendix E: Maps of data distribution, climatological mean temperature, and difference from annual mean for each monthly compositing period for selected standard depth levels.

